

Inhalable Textile Microplastic Fibers Impair Airway Epithelial Differentiation

Shanshan Song^{1,2#}, Fransien van Dijk^{1,2#}, Gwenda F Vasse^{1,2}, Qiongliang Liu³, Irene F Gosselink⁴, Ellen Weltjens⁴, Alex HV Remels⁴, Marina H de Jager¹, Sophie Bos¹, Chenxi Li³, Tobias Stoeger³, Markus Rehberg³, David Kutschke³, Gail van Eck¹, Xinhui Wu^{1,2}, Suzanne H Willems¹, Devin Boom⁵, Ingeborg M Kooter⁵, Diana Spierings⁶, Rene Wardenaar⁶, Matthew Cole⁷, Martijn C Nawijn^{2,8}, Anna Salvati⁹, Reinoud Gosens^{1,2}, Barbro N Melgert^{1,2,*}

¹Groningen Research Institute for Pharmacy, Department of Molecular Pharmacology, University of Groningen, Groningen, the Netherlands.

²Groningen Research Institute for Asthma and COPD, University Medical Center Groningen, University of Groningen, Groningen, the Netherlands.

³Comprehensive Pneumology Center, Institute of Lung Health and Immunity, Helmholtz Center Munich, German Research Center for Environmental Health, Neuherberg, Germany.

⁴School of Nutrition and Translational Research in Metabolism (NUTRIM), Department of Pharmacology and Toxicology, Maastricht University Medical Center+, Maastricht, the Netherlands.

⁵The Netherlands Organization for Applied Scientific Research, TNO, Utrecht, the Netherlands.

⁶European Research Institute for the Biology of Ageing, University Medical Center Groningen, University of Groningen, Groningen, the Netherlands.

⁷Plymouth Marine Laboratory, Plymouth, United Kingdom.

⁸Department of Pathology and Medical Biology, University Medical Center Groningen, University of Groningen, the Netherlands.

⁹Groningen Research Institute for Pharmacy, Department of Nanomedicine & Drug Targeting, University of Groningen, Groningen, the Netherlands.

Co-first author

* Corresponding author:

Prof Dr Barbro N. Melgert

Groningen Research Institute of Pharmacy

Department of Molecular Pharmacology

University of Groningen

A. Deusinglaan 1, 9713 AV Groningen

the Netherlands

b.n.melgert@rug.nl

ORCID: 0000-0001-7091-907X

Author contributions: SS, FD, GFV, and BNM: Study design, manuscript writing, collection of data, and data analysis. QL, IFG, EW, MHJ, SB, CL, DK, GE, SHW, DB, DS, and RW: Collection of data, and data analysis. AHVR, TS, MR, XW, IMK, MC, MCN, AS, and RG: Experimental support, critical reading and revision. All authors contributed to interpretation of data and manuscript preparation.

Funding: Dr Melgert/Gosens/Salvati/Cole/van Dijk received funding from ZonMw (Microplastics and Health grant 458001013). Dr Melgert/Song/Vasse/Kooter/Remels/Gosselink received funding from ZonMw (Health Holland consortium grant MOMENTUM 458001101).

Running head: Nylon inhibits airway epithelial differentiation

Descriptor: 6.2 Air Pollution: Mechanisms

Word Count: 5252

At a Glance Commentary

Current scientific knowledge on the subject:

Microplastics are present in the air we breathe and have been found in lung tissue. Experimental studies on animals have demonstrated microplastic-induced inflammatory responses and histological changes in lungs, while epidemiological studies have suggested links between airborne microplastics and respiratory health issues in humans. Especially studies on occupational exposures have shown that 15-40% of workers exposed to synthetic fibers develop work-related airway and interstitial lung disease. However, a comprehensive understanding of the biological mechanisms underlying these associations remains elusive.

What this study adds to the field:

The goal of the present study was to investigate if and how inhalable microplastics could affect epithelial repair mechanisms. Using a combination of murine and human lung organoids, experimental animals and air-liquid interface cultures, we demonstrate that nylon microplastic fibers inhibit airway epithelial differentiation, thereby interfering with lung repair processes, through transcription factor Hoxa5. A still unknown chemical leaching from nylon was found to be responsible for these effects. Our results are a first step towards generating data for risk assessment and establishing much-needed safe exposure levels in humans.

Some of the results of these studies have been previously reported in the form of a preprint (bioRxiv, 9 March 2021, www.biorxiv.org/content/10.1101/2021.01.25.428144v3).

This article has an online data supplement, which is accessible from this issue's table of content online at www.atsjournals.org.

Abstract

Rationale

Microplastics are a pressing global concern and inhalation of microplastic fibers has been associated with interstitial and bronchial inflammation in flock workers. However, how microplastic fibers affect the lungs is unknown.

Objectives

Our aim was to assess the effects of 12x31 μm nylon 6,6 (nylon) and 15x52 μm polyethylene terephthalate (polyester) textile microplastic fibers on lung epithelial growth and differentiation.

Methods

We used human and murine alveolar and airway-type organoids as well as air-liquid interface cultures derived from primary lung epithelial progenitor cells and incubated these with either nylon or polyester fibers or nylon leachate. In addition, mice received one dose of nylon fibers or nylon leachate and 7 days later organoid-forming capacity of isolated epithelial cells was investigated.

Results

We observed that nylon microfibers, more than polyester, inhibited developing airway organoids and not established ones. This effect was mediated by components leaching from nylon. Epithelial cells isolated from mice exposed to nylon fibers or leachate, also formed fewer airway organoids, suggesting long-lasting effects of nylon components on epithelial cells. Part of these effects were recapitulated in human air-liquid interface cultures. Transcriptome analysis revealed upregulation of *Hoxa5* post-exposure to nylon fibers. Inhibiting *Hoxa5* during nylon exposure restored airway organoid formation, confirming *Hoxa5*'s pivotal role in the effects of nylon.

Conclusions

These results suggest that components leaching from nylon 6,6 may especially harm developing airways and/or airways undergoing repair and we strongly encourage to characterize both hazard of and exposure to microplastic fibers in more detail.

Key words: Lung epithelial repair, Airway organoids, Polyester, Polyethylene terephthalate, Nylon

Abstract word count: 247

Introduction

Plastic pollution is a pressing global concern and microplastics are a significant part of this problem (1, 2). High amounts of microplastics have been found in marine environments, air, soils, plants and animals, which illustrates how omnipresent this pollutant is (3, 4). Microplastics can enter the human body via ingestion, dermal contact, and/or inhalation. Confirmation of human exposure was shown in a recent study by Leslie *et al.* that showed an average of 1.6 µg/ml of plastic in human blood (5).

Synthetic textile fibers are the most prevalent type of microplastic observed in indoor air (6–10) and levels indoors generally are 2-5 times higher than outdoors (11, 12). These fibers are typically composed of polyester or nylon and are released into the environment by wear and tear and during washing and drying of garments (13). The ubiquitous nature of microplastics indoors is unavoidably leading to human exposure via inhalation. Indeed, presence of microplastic fibers in human lung tissue was shown in three separate studies (14–16), with polyester being the most commonly identified polymer. Furthermore, combinations of degraded and fragmented textile fibers, with an average size of almost 2 µm, were found in bronchoalveolar lavage fluid samples, suggesting that large textile fibers are also able to reach the lower airways (17). Studies from workers in synthetic textile, flock and polyvinyl chloride industries indicate that inhalation of levels of around 7 mg/m³ or 1 million fibers/m³ of such microfibers can be harmful (18). Up to 40% of factory workers were found to develop work-related airway and interstitial lung disease (19, 20).

Unfortunately, health effects of long-term exposure to inhaled microplastics are greatly understudied and explanations for the effects in plastic industry workers are lacking. In this study, we therefore investigated effects of long-term exposure to nylon and polyester microfibers on growth and differentiation of lung epithelial cells using a murine and human lung organoid model, human air-liquid interface cultures, and a mouse model of fiber exposure. To extend the applicability of our

findings, we investigated both standardized and environmentally relevant fibers. These ranged from uniform, well-defined nylon 6,6 (nylon) and polyethylene terephthalate (polyester) fibers to fibers generated from locally sourced undefined nylon and polyester fabrics and irregularly shaped nylon particles generated within the Momentum consortium (momentummicroplastics.nl) by grinding and sieving of larger pieces of nylon.

Some of the results of these studies have been previously reported in the form of an abstract (21, 22).

Materials and Methods

Full experimental details are available in the data supplement.

Production of fibers and leachate

Microfibers of standardized dimensions and Nile red-labeled nylon were produced as described before (23) from polyethylene terephthalate (ES305710, Goodfellow, UK) or nylon 6,6 (AM325705, Goodfellow). Environmental polyester and nylon microfibers were prepared from commercially available fabrics. Microfibers were characterized using scanning electron microscopy and dimensions were determined as described in the data supplement. Nylon leachate was produced by incubation of nylon in phosphate buffered saline (PBS) for 7 days at 37°C. Leachate was characterized by mass spectrometry as described in the data supplement. Nylon microplastic particles in sizes 1-5 µm and 5-10 µm were supplied by the Momentum consortium (<https://momentummicroplastics.nl>).

Estimation of exposure concentrations

Exposure concentrations were extrapolated from occupational exposures of around 7 mg/m³ (18), a deposition efficiency of around 20% for cylindrical particles (24), and the assumption that a factory worker would inhale around 8000 liters of air per 8-hour shift (25). Assuming a perfect distribution

over a pair of lungs of around 1 kg would result in a concentration of around 11 $\mu\text{g/g}$ of lung tissue *each day*, corresponding to roughly 11 $\mu\text{g/ml}$ of culture medium in organoid cultures. We therefore investigated 2000-5000 fibers per well of organoids corresponding to 16-39 $\mu\text{g/ml}$ of nylon and 49-122 $\mu\text{g/ml}$ polyester. For the Momentum nylon particles (momentummicroplastics.nl) we tested 1, 10, and 100 $\mu\text{g/ml}$.

Animal experiments

All experiments were performed according to strict governmental and international guidelines on animal experimentation under licenses IVD 15303-01-004 (Groningen) and ROB-55.2Vet-2532.Vet_02-19-150 (Munich). C57BL/6 mice (males and females, 8-14 weeks) for organoid experiments were bred at the central animal facility of the University Medical Center Groningen. Female C57BL/6 mice for *in vivo* exposure experiments were purchased from Charles River (Sulzfeld, Germany). These mice received an intratracheal instillation of Nile red-labeled nylon or unlabeled nylon fibers or leachate suspended in 50 μl PBS containing 0.05% bovine serum albumin. After 7 days, mice were sacrificed and lung tissues were collected for lung organoid cultures.

Human lung tissue

Epithelial cells for organoids were isolated from nontumorous lung tissue anonymously donated by individuals with or without COPD undergoing surgery for lung cancer or lung transplantation for COPD and not objecting to the use of their tissue. Primary bronchial epithelial cells for air-liquid interface cultures were isolated from resected lung tissue from non-COPD patients or healthy tracheal-bronchial tissue donors. Known clinical characteristics of all patients are listed in table 1. The study protocols were consistent with the Research Code of the UMCG or the scientific board of the Maastricht Pathology Tissue Collection and the local Medical Ethics Committees, as well as with Dutch national ethical and professional guidelines (www.federa.org).

Lung organoid cultures

Lung organoids were grown from primary human or mouse lung CD31⁻CD45⁻Epcam⁺ cells co-cultured with human MRC5 or mouse CCL206 fibroblasts as previously described with minor modifications (26, 27). For most experiments, 5000 polyester or nylon reference or environmental microfibers were used per condition. Fibers were directly mixed in with Matrigel/cell suspensions, added on top of Matrigel, or equivalent amounts of fiber leachate or 5 μ M LE135 (TOCRIS #2021) were added to the medium during organoid culture. The number and size of organoids was manually quantified using a light microscope (Nikon, Eclipse Ti), only including organoids larger than 50 μ m in diameter.

Human airway organoids (27, 28)

20,000 human CD31⁻CD45⁻Epcam⁺ cells were resuspended with 5000 nylon fibers in droplets of 50 μ l growth factor reduced BME2 (R&D #3533-010-02) and added on pre-warmed 24-well suspension culture plates (Greiner #M9312) with 500 μ l of airway organoid medium with or without 2.5 μ M LE135 per well (28). After 21 days, the total number and the size of organoids was quantified, only including organoids larger than 100 μ m in diameter.

Air-liquid interface (ALI) cultures

Primary bronchial epithelial cells were seeded in coated transwell inserts, grown submerged until reaching 95% confluency and subsequently airlifted and cultured for 26-32 days. ALI cultures were continuously exposed to 40-50 μ g/ml nylon microfibers starting either one day after seeding or upon airlifting. Transepithelial electrical resistance was monitored at an approximately 7-day interval.

PCR

Total RNA was extracted from ALI cultures that were exposed to 40 μ g/ml nylon microfibers starting one day after seeding and cultured at air-liquid interface for 26 days. RNA was reverse transcribed into cDNA for real-time quantitative PCR. Gene expression levels of keratin 5, P63, FoxJ1 and Scgb1a1

were normalized to the average expression of housekeeping genes cyclophilin A and RPL13A by using the 2^{-ddCt} method.

Histology

Organoid cultures in Matrigel were stained for ACT and pro-SPC with primary antibodies as described previously (26). Isolated organoids and ALI cultures were stained using immunohistochemistry for P63, ACT and Scgb1a1 (organoids and ALI cultures), ProSPC and Ki67 (organoids) and FoxJ1 (ALI cultures) according to sample- and antibody-specific protocols.

Isolation of epithelial cells and fibroblasts from organoid cultures and RNA sequencing

Epcam⁺ (epithelial cells) were isolated from fresh lung tissue and 7-day old organoid cultures using anti-Epcam microbeads. These were used together with the Epcam⁻ (fibroblasts) cells from 7-day old organoid cultures for RNA isolation and subsequent RNA sequencing as previously described (29). The RNAseq data have been deposited to the Gene Expression Omnibus GEO with dataset identifier GSE238065.

Data analyses

For RNA sequencing data, principal component analyses were performed in R using the R package DESeq2 (version 1.26.0) to visualize the overall effect of experimental covariates as well as batch effects (function: plotPCA). Differential gene expression analyses (treated vs. nontreated) were performed with the same R package (default settings; Negative Binomial GLM fitting and Wald statistics; design= \sim mouse+condition), following standard normalization procedures. Genes with differential expression >2 (nylon-treated versus nontreated epithelial cells or fibroblasts) and a false discovery rate (FDR) smaller than 0.05 were considered differentially expressed for that specific cell type. Volcano plots were made in R studio using ggplot2 and clustering heat maps were made using BioJupies. Pathway analysis was done using Metascape. Cellular deconvolution of bulk RNA sequencing data from Epcam⁺ cells was done using MuSIC (30) with a single cell sequencing dataset

from Angelidis *et al.* (31) for freshly isolated epithelial cells and a dataset from Choi *et al.* (32) for epithelial cells isolated from 7-day organoid cultures.

Statistics

Statistical analyses were performed in either GraphPad Prism 9.0 or in R studio (R Studio 2022.02.2+485 "Prairie Trillium" Release). For data $n < 8$ nonparametric testing was used to compare groups, whereas for $n > 8$ parametric testing was used if data were normally distributed as assessed from QQ plots. For comparison of multiple groups, a Kruskal Wallis or Friedman test was used for nonpaired or paired nonparametric data respectively, with Dunn's correction for multiple testing, or a paired/unpaired one-way ANOVA for parametric data with Sidak's correction for multiple testing. Differences in organoid size between groups were tested by using the average size of the organoids per independent replicate. Data are presented as median \pm range and p-values < 0.05 were considered significant.

Results

Nylon microfibers inhibit growth of murine lung organoids

Fibers (aspect ratio 3:1) with a median size of $15 \times 52 \mu\text{m}$ for polyester and $12 \times 31 \mu\text{m}$ for nylon (Figure 1A) were extensively characterized (Figure E1, Table E1) before use in organoid cultures (Figure 1B). Based on pilot results (Figure E2), we exposed organoids to 5000 polyester or nylon fibers per well (equivalent to $122 \mu\text{g/ml}$ polyester or $39 \mu\text{g/ml}$ nylon). This concentration was conceivable in occupational exposure situations, had clear effects, and was on the lower end of the spectrum of concentrations used in other studies (33). Murine lung organoids commonly develop into ACT⁺ airway organoids or pro-SPC⁺ alveolar organoids and 14-day exposure to either polyester or nylon fibers resulted in significantly fewer and smaller organoids compared to control (Figure 1C-G). The inhibitory

effect of nylon was most profound on airway organoids. (Figure 1E-G). In addition, we tested nylon 6,6 particles from the Dutch Momentum research consortium (<https://momentummicroplastics.nl/>) and found these irregular sphere-shaped particles to be inhibitory in concentrations as low as 1 µg/ml (Figure E3). This demonstrated that the harmful effects of nylon fibers are also present at much lower doses and with differently shaped nylon.

To exclude cytotoxicity as a cause, we first assessed viability of primary epithelial cells in the presence of 39 µg/ml of nylon fibers or leachate and found no effects on the metabolic activity/proliferation of these cells (Figure E4A). Furthermore, the number and size of developing organoids during the survival and proliferation phase of organoids at day 7 was not affected by nylon (Figure E4B). These results all suggest that nylon is not directly cytotoxic.

Nylon microfibers inhibit growth of human lung organoids

Similar results were observed in human lung organoids, that mainly develop into alveolar organoids or mixed alveolar/airway organoids (Figure 2A-B). Exposure to nylon fibers resulted in significantly fewer human lung organoids, whereas the effects of polyester were less profound (Figure 2C-D). Organoid size was not affected by the presence of fibers. To further confirm effects on airway development, we specifically tested nylon on dedicated human airway organoids (Figure 2E-F). Again, we found that nylon significantly inhibited the number of organoids but had no effects on size (Figure 2G). As lung tissue was mostly obtained from patients with COPD, we assessed whether having COPD influenced the effects of microplastics exposure. We compared outcomes of cultures from COPD gold stage IV with cultures from no COPD/mild COPD (GOLD stage I and II) and found no differences in outcomes when treated with or without microplastics (data not shown).

Environmental microplastic fibers also impair lung organoid growth

To test if environmentally-relevant polyester and nylon fibers had similar effects as pristine fibers, we also tested fibers made from textile fabrics on murine lung organoids. We first characterized morphology (Figure 3A) and chemical composition of these environmental fibers (Figure E5). For polyester, we observed a median size of 17x63 μm (Table E2) and for nylon a median size of 57x20 μm (Table E2). Similar to reference fibers, 14-day exposure to 5000 environmental nylon fibers resulted in significantly fewer and smaller airway and alveolar organoids, while the effect of polyester was again less profound (Figures 3B-D).

Nylon leachate causes a reduction in lung organoid growth

We then investigated whether the inhibition by nylon was caused by interactions of cells with fibers or by leaching components from nylon. Pristine nylon microfibers were added to organoid cultures either in or on top of the Matrigel or equivalent amounts of nylon fiber leachate were added to organoid medium (Figure 4A). Both the presence of nylon microfibers on top of the Matrigel as well as leachate resulted in significantly fewer and smaller airway organoids compared to control. This was not the case for alveolar organoids, that increased significantly in number with nylon leachate (Figure 4B-D). These data suggest that airway epithelial growth is specifically inhibited by components leaching from nylon but alveolar epithelial growth may not be.

The strong effects observed with nylon leachate suggested that some components and/or degradation products may leak and/or form during culture. Mass spectrometry analysis revealed high concentrations of cyclic nylon oligomers in the leachate (Figure E6A). However, 53.6 $\mu\text{g}/\text{ml}$ of these oligomers separately or in combination had no effects on either number or size of organoids (Figure E6B). In addition, PEG600 was detected in leachate, but 1 μM up to 10 mM also did not affect outgrowth of organoids (Figure E6C). Recent studies showed the most abundant chemicals leaching from nylon in sea water were bisphenol A and benzophenone-3 (10, 33) . However, we could not detect these in our leachate and importantly, preliminary experiments with different concentrations

of bisphenol A (2 ng/ml-2000 ng/ml) or benzophenone-3 (1 nM-10 mM) showed no effects on lung organoid growth (Figures S6D-E).

Nylon leachate mainly affects airway epithelial differentiation

We then investigated if nylon fibers affect developing or established organoids differently. Lung organoid cultures have a clearly defined survival and proliferation phase (day 0 to 7), a differentiation phase (day 7 to 14), and an established phase (>14 days) (34) (Figure 5A). In contrast to the strong effects observed for developing organoids, we found that fibers on top of the Matrigel or leachate had no effects on established organoids (Figure 5B and Figure E7A for representative pictures of the cultures). However, organoid cultures exposed to nylon leachate or fibers on top of the Matrigel during the differentiation phase from day 7 to 14 also contained fewer airway organoids. No effects on size were found (Figure E7B,C). This suggests that nylon leachate specifically inhibits differentiation of airway epithelial cells and is not directly toxic to cells.

To elucidate how differentiation was affected by nylon, we investigated several markers of differentiation and proliferation in 14-day control and nylon-exposed organoids (Figure 5C). Visually the cultures were different with many more big and hollow organoids (airway-like structures) with multilayer walls in control cultures than in nylon-treated cultures. The latter contained more smaller clump-like structures (alveolar-like structures) and the airway-like organoids tended to be smaller, more branched/disorganized and with thinner walls. We stained sections of these organoid cultures for several markers that indicate differentiation to more terminally differentiated epithelial cell types: p63 for basal cells, acetylated alpha-tubulin (ACT) for ciliated cells, secretoglobin family 1A member (Scgb1a1, also known as CC10) for club cells, and prosurfactant C (pro-SPC) for type II cells. Additionally, we also stained for proliferation marker Ki67 to again exclude effects of nylon on proliferation of cells. The hollow airway-like organoids in control cultures clearly expressed airway markers P63, ACT, and Scgb1a1 and not alveolar marker pro-SPC. The branched and thinner-walled airway-like organoids in nylon-treated cultures contained fewer cells expressing ACT and Scgb1a1 and

no expression of pro-SPC. P63 expression was abundantly present in nylon-treated organoids (in both airway and alveolar-like organoids) but was more present in the cytoplasm of cells and less localized to the nucleus compared to control organoids. In addition, the more clump-like alveolar-like structures did not express either acetylated alpha-tubulin or *Scgb1a1* but did express pro-SPC in some structures. Lastly, in both control and nylon-treated cultures we found Ki67-positive proliferating cells, with no obvious differences between the two conditions. This again confirmed nylon was not inhibiting proliferation on day 14 of culture.

We then also investigated the effects of nylon leachate on human airway epithelial differentiation in ALI cultures of primary bronchial epithelial cells. Basolateral exposure of these cultures to 40-50 µg/ml nylon fibers, either one day after seeding or upon airlifting, resulted in thinner epithelial layers, but only in donors that developed well in untreated control conditions, highlighting interdonor variability (Figure 5D). Both treatment strategies did not affect transepithelial resistance in a negative way (Figure E7D). We then stained a well-developed and a less-developed donor, that were exposed to nylon upon airlifting, for airway epithelial markers. After nylon exposure, only the well-developed donor had less staining for ciliated cells (ACT and FOXJ1), basal cells (P63+) and club cells (*Scgb1a1*), again indicating that to visualize effects of nylon, cells in control conditions need to be differentiating well (Figure 5E and Figure E8). In addition, we found more mRNA expression of basal cell markers keratin 5 (*Krt5*) and P63 (*Trp63*), less expression of ciliated cell marker *Foxj1* and no changes in club cell marker *Scgb1a1* in cultures exposed from the start (Figure E7E). Summarizing, treatment with nylon does not impair epithelial proliferation but specifically inhibits differentiation to more terminally differentiated airway epithelial cells.

Exposure to nylon inhibits airway epithelial developmental pathways and stimulates expression of Hox family genes

To better understand the mechanisms behind the observed effects on epithelial differentiation, we performed bulk RNA-sequencing analysis on freshly isolated epithelial cells and epithelial cells and

fibroblasts isolated from 7-day organoid cultures exposed to 2k or 5k nylon fibers. This time point was chosen to capture transcriptomic changes before cellular composition changes had set in.

Cellular deconvolution of bulk RNAseq data from freshly isolated epithelial cells showed that around 70% of epithelial cells going into the organoid assay were type II epithelial cells, $\pm 15\%$ were ciliated cells and, $\pm 10\%$ were type I epithelial cells (Figure E9A), which was consistent with data using flow cytometry to identify cell types (35). After 7 days of organoid culture these identities had changed dramatically to around 70% proliferating epithelial cells and 30% alveolar intermediates positive for keratin 8 (Figure 6A). The latter can differentiate into alveolar epithelial cells after damage *in vivo* (36). Treatment with 2000 nylon fibers did not affect those proportions, but treatment with 5000 nylon fibers resulted in fewer alveolar intermediates and a concomitant increase in stromal cells. This may be an indication of epithelial-to-mesenchymal transition (EMT) of these epithelial cells because they were positively selected for Epcam and were therefore unlikely to be fibroblasts. We investigated expression of EMT markers N-cadherin (Cdh2), vimentin (Vim), T-Box transcription factor 3 (Tbx3), snail family transcriptional repressor 2 (Snai2), Twist1 (Twist family BHLH transcription factor 1), and Acta2 (α -SMA) and found all of them to be expressed at higher levels in organoids treated with 5000 nylon fibers, while expression of epithelial adhesion marker E-cadherin (Cdh1) was lower (Figure E9B). All of which points at development of EMT (37).

Both concentrations of nylon had an enormous impact on epithelial gene expression as depicted in volcano plots (Figures 6B,C) and unsupervised clustering heat maps (Figure E9C). Pathways for downregulated genes were highly enriched for epithelial development and function, while those identified for upregulated genes were highly enriched for mRNA translation and protein synthesis (Figure 6D,E, see supplemental data tables 4 and 5 for full list of pathways).

We then investigated the expression of individual genes in both top-5 enriched pathways in more detail. Many of the downregulated genes represent important epithelial populations in the lung. The genes associated with specific epithelial populations are listed in table E3. The expression of these genes correlated well with our histological findings that airway epithelial cells were most affected by exposure to nylon fibers, while alveolar epithelial cell growth was less affected (Figure 6F,G). Proliferation markers in epithelial cells were not greatly affected, confirming nylon mainly affects epithelial differentiation and not proliferation (Figure 6H). Expression of genes for signaling molecules essential for epithelial differentiation and growth were also dose-dependently downregulated by nylon (Figure E9D). The genes prominently upregulated after nylon exposure were mostly encoding for ribosomal proteins including Rpl38 (Figure E9E), which regulates expression of homeobox (*Hox*) genes that are important for cell and tissue identities (38). Interestingly, *Hoxa4*, *Hoxa5*, *Hoxc9*, and *Hoxb3* were all significantly higher after nylon exposure (Figure 6I), with *Hoxa5* being most profoundly induced.

To exclude the possibility that these effects on epithelial cells were mediated by fibroblasts, we separately analyzed the resorted fibroblast fraction for expression of proliferation genes and important growth factors. None of these genes were inhibited by nylon in fibroblasts (Figure E10A-B).

***Hoxa5* inhibitor LE135 restores airway organoid formation in the presence of nylon**

To confirm RNA data, we investigated protein expression of *Hoxa5* in organoids. *Hoxa5* protein was highly expressed in many epithelial organoids (Figure 7A) and most nuclei of nylon-exposed organoids but hardly expressed in control organoids (Figure 7B). To further assess the role of *Hoxa5* in defective airway epithelial development, we used a *Hoxa5* inhibitor (LE135), a retinoic acid receptor β -specific antagonist, which inhibits retinoic acid-induced *Hoxa5* expression (39). Our data showed that exposure to LE135 in presence of nylon rescued the development of murine airway organoids (Figure

7C,D). In addition, we found similar effects in human airway organoids (Figure 7E,F). These results indicate that nylon inhibited differentiation of airway organoids through *Hoxa5*.

***In vivo* exposure of mice to nylon fibers results in long-lasting inhibition of airway epithelial differentiation as assessed by organoid formation**

To investigate the effects of nylon on lung epithelial repair, we exposed mice once to either 75k or 150k fibers or leachate and we isolated lung epithelial cells after seven days for organoid culture (Figure 8A). *Ex vivo* fluorescence imaging on excised lungs of mice exposed to labeled nylon fibers revealed that 3 days after exposure many fibers were still present in all areas of the lung. Seven days after exposure some fibers were obviously cleared and the remaining ones had accumulated centrally (Figure 8B). Nylon treatment did not result in body weight loss (Figure E11). The number of airway organoids growing from these *in vivo*-exposed mice was significantly lower than for control exposure, indicating that being exposed once to nylon fibers or its leachate *in vivo* is sufficient for long lasting inhibition of cell differentiation (Figure 8C,D). Nylon exposure did not affect the number of alveolar organoids (Figure 8C,E). To investigate whether *Hoxa5* inhibition could alleviate the effects of *in vivo* nylon exposure, we treated organoid cultures from either vehicle or nylon exposed mice with LE135 for 14 days (Figure 8C-E). This resulted in significantly more, but smaller, airway organoids compared to untreated organoid cultures derived from nylon or nylon leachate-exposed mice (Figure 8D and Figure E12A,C). The number of alveolar organoids was lower and their size was smaller after LE135 treatment (Figure 8E and Figure E12B,D).

Discussion

Recent reports have shown that man-made fibers are ubiquitously present in indoor air (6, 11, 40, 41). We are therefore continuously exposed to this airborne microplastic pollution (40), but the consequences of common household exposure on our lungs are unclear. Evidence from textile factory workers indicate detrimental effects on lung tissue during high exposure conditions at levels of around

7 mg/m³ or 1 million fibers/m³ (18). Our data now show that both polyester and nylon fibers can impair differentiation of human and murine lung epithelial cells, with nylon being the most harmful for airway epithelial cell differentiation. The effects of polyester were much milder and confirm previous findings by *Winkler et al* demonstrating that lower concentrations of polyester microplastics (50 µg/ml) had no effects on human airway organoid growth (27). The effects of nylon were mediated by compounds leaking from nylon that upregulate *Hoxa5*, which in turn specifically inhibits differentiation of airway epithelial cells.

Components leaching from nylon were found to be consistently harmful for growth of airway organoids rather than alveolar organoids, which may explain the bronchiolitis found in nylon flock workers and rats exposed to nylon (42–44). Since we were unable to identify the specific culprit(s) responsible for this effect of nylon, we concentrated on elucidating the pathway responsible for the observed inhibition of airway development and found a role for *Hoxa5*. Our data suggest upregulation of *Hoxa5* in epithelial cells inhibits terminal differentiation of airway epithelial cells and instead keeps them in an aberrant basal phenotype with EMT characteristics. These findings are supported by work from *Fujino et al.* showing that increased expression of *Hoxa5* drives EMT in alveolar epithelial cells (45), *Yang et al.* and *Yao et al.* showing that nylon enhances EMT (46–48) and *Boucherat et al.* showing that loss of *Hoxa5* drives epithelial differentiation towards goblet cells (49). Therefore, upregulation of *Hoxa5* in epithelial cells by nylon appears to be a determining factor in the impairment of airway organoid differentiation and this finding was confirmed when we inhibited *Hoxa5* and found restoration of airway organoid development. As stromal cells are also known to express *Hoxa5*, the *Hoxa5* upregulation with downstream effects we found, could theoretically also be caused by the fibroblasts present in the mixed lung organoid cultures. However, we think this is an unlikely explanation for the following reasons: 1. The growth-inhibited fibroblasts present in murine organoid cultures expressed *Hoxa5*, but this expression was actually downregulated by nylon, while nylon upregulated *Hoxa5* expression in epithelial cells. 2. Even human airway organoid cultures that were

grown without fibroblasts present, were inhibited by nylon and rescued by Hoxa5 inhibitor LE135. Incidentally, the inhibition of Hoxa5 also resulted in fewer and smaller alveolar-like organoids. Our hypothesis for this finding is that inhibition of Hoxa5 allows more progenitors to develop towards airways and that this may reduce the number available for alveolar development.

Whether nylon components directly or indirectly upregulate Hoxa5 remains an open question. The upregulation of Hoxa5 may also be the result of inhibition of Wingless/Integrated (Wnt) signalling by nylon components. Ordóñez-Morán *et al.* previously showed a feedback loop between Hoxa5 and Wnt in intestinal stem cells, with Wnt signalling suppressing Hoxa5 expression to maintain stemness (50). Therefore, inhibition of Wnt family members by nylon components could indirectly result in upregulation of Hoxa5. Support for this hypothesis is found in our RNAseq data, which showed downregulation of both Wnt4 and Wnt7 concomitant to upregulation of Hoxa5 by nylon.

Our data uniquely show that nylon fibers especially inhibit differentiating (airway) epithelial cells. However, nylon did not affect already developed airway organoids or proliferation of epithelial cells. This suggests that nylon is not directly toxic, but that it only interferes with developmental and/or repair pathways. It is therefore likely that the potential adverse health effects of nylon are especially relevant for young children with developing airways and patients with chronic or acute lung disease, who rely on epithelial repair. Recent studies have already shown potential health impacts of microplastics in early life and patients with asthma (51, 52). Of note, a recent study by Soltani *et al.* estimated possible household exposure in different types of individuals and found that young children (<0.5 years of age) could inhale twice as much microplastics as adults, averaging 45 ng per kg of bodyweight per day (12). In addition, microplastics were shown to be present in human placenta and in mice this resulted in reproductive toxicity (53, 54). Therefore, the presence of inhalable microplastic/nylon fibers in indoor environments is a matter of great concern for children/fetuses who still grow their lungs.

Nevertheless, this concern is only relevant when concentrations of these fibers are high enough to cause adverse effects and this is where data are severely lacking. Studies have shown microplastic fibers to be ubiquitously present in houses with an average of 5 fibers per m³ of air (8, 55), but actual lung deposition of these microplastic fibers has not been quantified yet. Vianello *et al.* used a breathing thermal manikin to estimate adult human lung deposition by inhalation in daily life (40). They showed that on average 9 particles per m³ of air were inhaled by this device. As humans process around 11 m³ of air per day, exposure could be around 100 particles per day. This is similar to estimations in Australian homes of around 13,000 fibers per year (12). Another comprehensive review estimated that annual inhalation of microplastic particles could be between 40,000 and 62,000 particles/year (56). However, this may be an underestimation as high exposure activities like unloading a tumble drier, working with textile materials, or crawling around on carpets were not considered. Neither were ventilation habits considered and these factors could all greatly determine exposure, although vacuum cleaning was estimated to reduce exposure (12). Therefore, microplastic concentrations in indoor environments need to be assessed more widely during a variety of activities and conditions to make better estimations of human exposure possible. These can then be compared to occupational exposures known to cause adverse effects and animal studies such as ours and previous ones (42, 44). For instance, concentrations of 7 mg/m³ or 10⁶ fibers per m³ air were found in the nylon flocking industry with many employees reporting respiratory symptoms (18, 57). Furthermore, rats exposed once to 10 mg/kg bodyweight developed bronchiolitis (42), but 4-week exposure to 57 fibers/cm³ did not lead to adverse effects in rats (44).

A strength of using lung organoids is the opportunity to directly translate *ex vivo* findings to humans (27, 58). As we found comparable negative effects of nylon fibers on epithelial differentiation and growth in murine and human organoids, this demonstrates our results are of high relevance for the human population. Despite this advantage, lung organoids are a relatively simple model of lung tissue

and lack the immune and endothelial compartment present *in vivo*. Especially having the immune cells present could alter how lung tissue responds to these microplastic fibers. For example, innate immune cells like macrophages are also among the first cells to come into contact with microplastic fibers following inhalation and can respond strongly to inhaled particles and fibers (59). Therefore, future studies should also focus on more complex models involving an immune component as well.

A limitation in our work is not having access to a specific Hoxa5 inhibitor. Even though inhibiting retinoic acid receptor beta with LE135 has a fairly specific effect on Hoxa5 expression (39), we cannot exclude the possibility other proteins were affected by this treatment and contributed to the effect.

In conclusion, as plastic use continues to expand, there may be a corresponding rise in health risks for humans. This study underscores the pressing need to delve deeper into the dangers and prevalence of microplastic fibers. Those outcomes will be invaluable to advisory organizations like the World Health Organization and Science Advice for Policy by European Academies who recently called for more data on effects of microplastics on human health (2). Future research endeavors should prioritize analyzing the concentration and prevalence of these fibers in indoor settings and within human lung tissues to provide a more accurate assessment of their potential threat to human health.

Acknowledgments

The authors thank Habibie, Jesse Mulder, Imco Sibum, Paul Hagedoorn and Anko Eissens (University of Groningen), Andreas W. Ehlers (University of Amsterdam) and Elena Höppener (TNO) for their technical assistance and ZonMw for their financial support with the Microplastics and Health grant 458001013 (Melgert/Gosens/Salvati/Cole) and the ZonMw/Health Holland consortium grant MOMENTUM (458001101, momentummicroplastics.nl) led by Prof. Dr. J. Legler and Prof. Dr. D. Vethaak and awarded to Melgert and Kooter among others. We also acknowledge Prof. Jeroen den

Hertog (Hubrecht Institute) for providing Noggin-producing cells and Dr. Calvin Kuo (University of Stanford) for providing R-spondin1-producing cells.

References

1. Vethaak AD, Legler J. Microplastics and human health. *Science (1979)* 2021;371:672–674.
2. World Health Organization. *Dietary and inhalation exposure to nano- and microplastic particles and potential implications for human health*. 2022.
3. Gasperi J, Wright SL, Dris R, Collard F, Mandin C, Guerrouache M, *et al*. Microplastics in air: Are we breathing it in? *Curr Opin Environ Sci Health* 2018;1:1–5.
4. Rochman CM. Microplastics research — from sink to source in freshwater systems. *Science (1979)* 2018;360:28–29.
5. Leslie HA, van Velzen MJM, Brandsma SH, Vethaak AD, Garcia-Vallejo JJ, Lamoree MH. Discovery and quantification of plastic particle pollution in human blood. *Environ Int* 2022;163:107199.
6. Zhang J, Wang L, Kannan K. Microplastics in house dust from 12 countries and associated human exposure. *Environ Int* 2020;134:105314.
7. Dris R, Gasperi J, Saad M, Mirande C, Tassin B. Synthetic fibers in atmospheric fallout: A source of microplastics in the environment? *Mar Pollut Bull* 2016;104:290–293.
8. Yao Y, Glamoclija M, Murphy A, Gao Y. Characterization of microplastics in indoor and ambient air in northern New Jersey. *Environ Res* 2022;207:112142.
9. Liao Z, Ji X, Ma Y, Lv B, Huang W, Zhu X, *et al*. Airborne microplastics in indoor and outdoor environments of a coastal city in Eastern China. *J Hazard Mater* 2021;417:126007.
10. Salthammer T. Microplastics and their Additives in the Indoor Environment. *Angewandte Chemie - International Edition* 2022;61:.
11. Gaston E, Woo M, Steele C, Sukumaran S, Anderson S. Microplastics Differ Between Indoor and Outdoor Air Masses: Insights from Multiple Microscopy Methodologies. *Appl Spectrosc* 2020;74:1079–1098.
12. Soltani NS, Taylor MP, Wilson SP. Quantification and exposure assessment of microplastics in Australian indoor house dust. *Environ Pollut* 2021;283:117064.
13. Browne MA, Crump P, Niven SJ, Teuten E, Tonkin A, Galloway T, *et al*. Accumulation of microplastic on shorelines worldwide: Sources and sinks. *Environ Sci Technol* 2011;45:9175–9179.
14. Pauly JL, Stegmeier SJ, Allaart HA, Cheney RT, Zhang PJ, Mayer AG, *et al*. Inhaled cellulosic and plastic fibers found in human lung tissue. *Cancer Epidemiol Biomarkers Prev* 1998;7:419–28.
15. Amato-Lourenço LF, Carvalho-Oliveira R, Júnior GR, dos Santos Galvão L, Ando RA, Mauad T. Presence of airborne microplastics in human lung tissue. *J Hazard Mater* 2021;416:126124.
16. Jenner LC, Rotchell JM, Bennett RT, Cowen M, Tentzeris V, Sadofsky LR. Detection of microplastics in human lung tissue using μ FTIR spectroscopy. *Science of the Total Environment* 2022;831:154907.
17. Baeza-Martínez C, Olmos S, González-Pleiter M, López-Castellanos J, García-Pachón E, Masiá-Canuto M, *et al*. First evidence of microplastics isolated in European citizens' lower airway. *J Hazard Mater* 2022;438:129439.
18. Wright SL, Kelly FJ. Plastic and Human Health: A Micro Issue? *Environ Sci Technol* 2017;51:6634–6647.
19. Atis S, Tutluoglu B, Levent E, Ozturk C, Tunaci A, Sahin K, *et al*. The respiratory effects of occupational polypropylene flock exposure. *European Respiratory Journal* 2005;25:110–117.
20. Eschenbacher WL, Kreiss K, Loughheed MD, Pransky GS, Day B, Castellan RM. Clinical Pathology Workshop Summary Nylon Flock – Associated Interstitial Lung Disease. *Am J Respir Crit Care Med* 1999;159:2003–2008.
21. Song S, Van Dijk F, Eck G, Wu X, Bos S, Boom D, *et al*. Inhalable textile microplastic fibers impair lung repair [abstract]. *ERJ Open Research*; 2022. p. 8,Suppl. 69.doi:10.1183/23120541.LSC-2022.69.
22. Van Dijk F, Van Eck G, Cole M, Salvati A, Bos S, Gosens R, *et al*. Exposure to textile microplastic fibers impairs epithelial growth [abstract]. *European Respiratory Society*; 2020. p. 56: 1972.doi:10.1183/13993003.congress-2020.1972.
23. Cole M. A novel method for preparing microplastic fibers. *Sci Rep* 2016;6:1–7.

24. Mohammad S. Islam¹, Md. Mizanur Rahman, Puchanee Larpruenrudee, Akbar Arsalanloo, Hamidreza Mortazavy Beni, Md. Ariful Islam, YuanTong Gu and ES. How Microplastics are Transported and Deposited in Realistic Upper Airways? *Physics of Fluids* 2023;0–26.
25. Pleil JD, Ariel Geer Wallace M, Davis MD, Matty CM. The physics of human breathing: flow, timing, volume, and pressure parameters for normal, on-demand, and ventilator respiration. *J Breath Res* 2021;15:.
26. Wu X, Bos IST, Conlon TM, Ansari M, Verschut V, van der Koog L, *et al.* A transcriptomics-guided drug target discovery strategy identifies receptor ligands for lung regeneration. *Sci Adv* 2022;8:1–15.
27. Winkler AS, Cherubini A, Rusconi F, Santo N, Madaschi L, Pistoni C, *et al.* Human airway organoids and microplastic fibers: A new exposure model for emerging contaminants. *Environ Int* 2022;163:107200.
28. Sachs N, Papaspyropoulos A, Zomer-van Ommen DD, Heo I, Böttinger L, Klay D, *et al.* Long-term expanding human airway organoids for disease modeling. *EMBO J* 2019;38:1–20.
29. Ng-Blichfeldt J-P, de Jong T, Kortekaas RK, Wu X, Lindner M, Guryev V, *et al.* TGF- β activation impairs fibroblast ability to support adult lung epithelial progenitor cell organoid formation. *American Journal of Physiology-Lung Cellular and Molecular Physiology* 2019;317:L14–L28.
30. Wang X, Park J, Susztak K, Zhang NR, Li M. Bulk tissue cell type deconvolution with multi-subject single-cell expression reference. *Nat Commun* 2019;10:.
31. Angelidis I, Simon LM, Fernandez IE, Strunz M, Mayr CH, Greiffo FR, *et al.* An atlas of the aging lung mapped by single cell transcriptomics and deep tissue proteomics. *Nat Commun* 2019;10:1–17.
32. Choi J, Park J-E, Tsagkogeorga G, Yanagita M, Koo B-K, Han N, *et al.* Inflammatory Signals Induce AT2 Cell-Derived Damage-Associated Transient Progenitors that Mediate Alveolar Regeneration. *Cell Stem Cell* 2020;27:366–382.e7.
33. Sørensen L, Groven AS, Hovsbakken IA, Del Puerto O, Krause DF, Sarno A, *et al.* UV degradation of natural and synthetic microfibers causes fragmentation and release of polymer degradation products and chemical additives. *Sci Total Environ* 2021;755:143170.
34. Ng-Blichfeldt JP, Schrik A, Kortekaas RK, Noordhoek JA, Heijink IH, Hiemstra PS, *et al.* Retinoic acid signaling balances adult distal lung epithelial progenitor cell growth and differentiation. *EBioMedicine* 2018;36:461–474.
35. Hu Y, Ng-Blichfeldt JP, Ota C, Ciminieri C, Ren W, Hiemstra PS, *et al.* Wnt/ β -catenin signaling is critical for regenerative potential of distal lung epithelial progenitor cells in homeostasis and emphysema. *Stem Cells* 2020;38:1467–1478.
36. Strunz M, Simon LM, Ansari M, Kathiriya JJ, Angelidis I, Mayr CH, *et al.* Alveolar regeneration through a Krt8+ transitional stem cell state that persists in human lung fibrosis. *Nat Commun* 2020;11:3559.
37. Rout-Pitt N, Farrow N, Parsons D, Donnelley M. Epithelial mesenchymal transition (EMT): A universal process in lung diseases with implications for cystic fibrosis pathophysiology. *Respir Res* 2018;19:1–10.
38. Taniguchi Y. Hox Transcription Factors: Modulators of Cell-Cell and Cell-Extracellular Matrix Adhesion. *Biomed Res Int* 2014;2014:1–12.
39. Chen H, Zhang H, Lee J, Liang X, Wu X, Zhu T, *et al.* HOXA5 acts directly downstream of retinoic acid receptor β and contributes to retinoic acid-induced apoptosis and growth inhibition. *Cancer Res* 2007;67:8007–8013.
40. Vianello A, Jensen RL, Liu L, Vollertsen J. Simulating human exposure to indoor airborne microplastics using a Breathing Thermal Manikin. *Sci Rep* 2019;9:8670.
41. Zhang Q, Zhao Y, Du F, Cai H, Wang G, Shi H. Microplastic Fallout in Different Indoor Environments. *Environ Sci Technol* 2020;54:6530–6539.
42. Porter DW, Castranova V, Robinson VA, Hubbs AF, Mercer RR, Scabilloni J, *et al.* Acute inflammatory reaction in rats after intratracheal instillation of material collected from a nylon flocking plant. *J Toxicol Environ Health A* 1999;57:25–45.
43. Sauler M, Gulati M. Newly Recognized Occupational and Environmental Causes of Chronic Terminal Airways and Parenchymal Lung Disease. *Clin Chest Med* 2000;73:543–562.

44. Warheit DB, Webb TR, Reed KL, Hansen JF, Kennedy GL. Four-week inhalation toxicity study in rats with nylon respirable fibers: rapid lung clearance. *Toxicology* 2003;192:189–210.
45. Fujino N, Kubo H, Maclewicz RA. Phenotypic screening identifies Axl kinase as a negative regulator of an alveolar epithelial cell phenotype. *Laboratory Investigation* 2017;97:1047–1062.
46. Yang B, Cao G, Cai K, Wang G, Li P, Zheng L, *et al.* VEGF-Modified PVA/Silicone Nanofibers Enhance Islet Function Transplanted in Subcutaneous Site Followed by Device-Less Procedure. *Int J Nanomedicine* 2020;Volume 15:587–599.
47. Li X, Yan S, Dai J, Lu Y, Wang Y, Sun M, *et al.* Human lung epithelial cells A549 epithelial-mesenchymal transition induced by PVA/Collagen nanofiber. *Colloids Surf B Biointerfaces* 2018;162:390–397.
48. Yan S, Li X, Dai J, Wang Y, Wang B, Lu Y, *et al.* Electrospinning of PVA/sericin nanofiber and the effect on epithelial-mesenchymal transition of A549 cells. *Materials Science and Engineering: C* 2017;79:436–444.
49. Boucherat O, Chakir J, Jeannotte L. The loss of Hoxa5 function promotes Notch-dependent goblet cell metaplasia in lung airways. *Biol Open* 2012;1:677–691.
50. Ordóñez-Morán P, Dafflon C, Imajo M, Nishida E, Huelsenken J. HOXA5 Counteracts Stem Cell Traits by Inhibiting Wnt Signaling in Colorectal Cancer. *Cancer Cell* 2015;28:815–829.
51. Lu K, Lai KP, Stoeger T, Ji S, Lin Z, Lin X, *et al.* Detrimental effects of microplastic exposure on normal and asthmatic pulmonary physiology. *J Hazard Mater* 2021;416:126069.
52. Sripada K, Wierzbicka A, Abass K, Grimalt JO, Erbe A, Röllin HB. A Children ' s Health Perspective on Nano- and Microplastics. *Environ Health Perspect* 2022;130:1–15.
53. Ragusa A, Svelato A, Santacroce C, Catalano P, Notarstefano V, Carnevali O, *et al.* Plasticenta: First evidence of microplastics in human placenta. *Environ Int* 2021;146:106274.
54. Hu J, Qin X, Zhang J, Zhu Y, Zeng W, Lin Y, *et al.* Polystyrene microplastics disturb maternal-fetal immune balance and cause reproductive toxicity in pregnant mice. *Reproductive Toxicology* 2021;106:42–50.
55. Xumiao L, Prata JC, Alves JR, Duarte AC, Rocha-Santos T, Cerqueira M. Airborne microplastics and fibers in indoor residential environments in Aveiro, Portugal. *Environmental Advances* 2021;6:100134.
56. Lee S, Kang KK, Sung SE, Choi JH, Sung M, Seong KY, *et al.* In Vivo Toxicity and Pharmacokinetics of Polytetrafluoroethylene Microplastics in ICR Mice. *Polymers (Basel)* 2022;14:.
57. J Burkhardt 1, C Piacitelli, D Schwegler-Berry WJ. Environmental study of nylon flocking process. *J Toxicol Environ Health A* 1999;57:1–23.
58. Fatehullah A, Tan SH, Barker N. Organoids as an in vitro model of human development and disease. *Nat Cell Biol* 2016;18:246–254.
59. Kuroda E, Ozasa K, Temizoz B, Ohata K, Koo CX, Kanuma T, *et al.* Inhaled Fine Particles Induce Alveolar Macrophage Death and Interleukin-1 α Release to Promote Inducible Bronchus-Associated Lymphoid Tissue Formation. *Immunity* 2016;45:1299–1310.

Tables

Table 1. Demographics and clinical characteristics of patients whose lung tissue was used for isolation of epithelial cells for organoids or air-liquid interface cultures.

Type	Sex (F/M)	Age (yr)	Smoking status	Pack-years (yr)	FEV1/FVC ratio	COPD GOLD stage
Lung tissue used for lung organoid cultures						
Non-COPD	0/1	68	ES	15	73	NA
COPD	2/4	62 (52-65)	CS/ES (1), CS (1), ES (4)	25 (15-58)	46 (21-58)	I (1), II (2), IV (3)
Lung tissue used for airway organoid cultures						
COPD	4/3	58 (54-61)	ES (7)	25 (14-32)	28 (21-30)	IV (7)
Lung tissue used for air-liquid interface cultures						
Non-COPD	0/2	73 (72-73)	ES	Unknown	75 (72-78)	NA
Healthy	3 unknown	Unknown	Unknown	Unknown	Unknown	NA

F/M: female or male; ES: exsmoking; CS: current smoking; FEV1/FVC: ratio between forced expiratory volume in 1 s (FEV1) and forced vital capacity (FVC); NA: not applicable. Values are median (interquartile range).

Figure legends

Figure 1. Effects of microplastic fibers on outgrowth of murine lung organoids.

(A) Morphology of microplastic fibers of standardized dimensions. Representative SEM micrographs of polyester microfibers (15x52 μm) and nylon microfibers (12x31 μm). (B) Murine lung organoid co-culture model: 5000 polyester or 5000 nylon fibers (equivalent to 122 $\mu\text{g}/\text{ml}$ polyester or 39 $\mu\text{g}/\text{ml}$ nylon) were mixed together with Epcam⁺ cells, CCL206 fibroblasts, and Matrigel. (C-D) Light microscopy images and fluorescence images of acetylated alpha-tubulin (ACT⁺) airway organoids (red) and prosurfactant C (pro-SPC⁺) alveolar organoids (green). Nuclei were counterstained with DAPI (blue). (E) Representative light microscopy images of the different treatment conditions. Yellow arrows indicate airway organoids, cyan arrows indicate alveolar organoids, and red and white arrows indicate polyester and nylon fibers respectively. (F-G) Quantification of numbers and sizes of airway and alveolar lung organoids following 14-day exposure (n=12). Groups were compared using a Friedman test with Dunn's correction for multiple testing. P<0.05 was considered significant.

Figure 2. Influence of microplastic fibers on outgrowth of human lung and airway organoids.

(A) Human lung organoid co-culture model. 5000 15x52 μm polyester or 5000 12x31 μm nylon fibers (equivalent to 122 $\mu\text{g}/\text{ml}$ polyester or 39 $\mu\text{g}/\text{ml}$ nylon) were mixed with CD31⁻CD45⁻Epcam⁺ cells, MRC5 fibroblasts and Matrigel. (B) The morphology of alveolar prosurfactant C (pro-SPC⁺) organoids (green) and mixed acetylated alpha-tubulin (ACT⁺)/pro-SPC⁺ organoids (orange) as shown by light and fluorescence microscopy. Nuclei were counterstained with DAPI (blue). (C) Representative light microscopy images of all treatment conditions. Cyan arrows indicate lung organoids. (D) Quantification of numbers and sizes of human lung organoids following 14-day exposure to either no microfibers, 5000 polyester, or 5000 nylon fibers (n=7). Groups were compared using a Friedman test with Dunn's correction for multiple testing. P<0.05 was considered significant. (E) Human airway organoid model: 5000 nylon fibers were mixed with CD31⁻CD45⁻Epcam⁺ cells and BME2 gel. (F)

Representative light microscopy images of control or nylon-treated airway organoids. Yellow arrows indicate airway organoids. (G) Quantification of numbers and sizes of human airway organoids following 21-day exposure (n=6). Groups were compared using a Wilcoxon test. P<0.05 was considered significant.

Figure 3. Influence of environmentally relevant textile fibers on growth of murine lung organoids.

(A) Morphology of environmental (environm.) microplastic fibers. Representative SEM micrographs of polyester microfibers (17x63 μm) and nylon microfibers (57x20 μm). (B) Representative light microscopy images of all treatment conditions. Yellow arrows indicate airway organoids, whereas cyan arrows indicate alveolar organoids. (C-D) Quantification of numbers and sizes of airway and alveolar organoids (n=6) following 14-day exposure to either no microfibers, 5000 polyester, or 5000 nylon microfibers (equivalent to 189 $\mu\text{g}/\text{ml}$ polyester or 531 $\mu\text{g}/\text{ml}$ nylon). Groups were compared using a Friedman test with Dunn's correction for multiple testing. P<0.05 was considered significant.

Figure 4. Impact of nylon microfibers or leachate on growth of murine lung organoids.

(A) Experimental scheme. 12x31 μm nylon microfibers were added in or on top of Matrigel, or leachate of these fibers was added to the basolateral medium (B) Representative light microscopy images of all treatment conditions. (C-D) Quantification of numbers and sizes of airway and alveolar organoids following either direct exposure to 5000 nylon microfibers (equivalent to 39 $\mu\text{g}/\text{ml}$) in Matrigel or indirect exposure (n=6). Groups were compared using a Friedman test with Dunn's correction for multiple testing. P<0.05 was considered significant.

Figure 5. Nylon leachate has no effect on established lung organoids but inhibits airway epithelial differentiation.

(A) Experimental scheme. Organoids were exposed at day 0, 7 or 14 to 12x31 μm nylon fibers/leachate for 7-21 days. (B) Quantification of numbers of airway and alveolar organoids following exposure to

no or 5000 nylon microfibers (equivalent to 39 $\mu\text{g}/\text{ml}$) or leachate for 7, 14, or 21 days ($n=6-12$). Groups were compared using a one-way ANOVA with a Holm-Sidak correction for multiple testing. $P<0.05$ was considered significant. (C) Representative images of immunohistochemical stainings for differentiation and proliferation markers expressed by control lung organoids and lung organoids exposed to nylon for 14 days. Positive staining is red and nuclei are blue. P63 = basal cell marker; ACT = acetylated alpha-tubulin: ciliated cell marker; Scgb1a1 = secretoglobin family 1A member: club cell marker; Pro-SPC = prosurfactant C: Type II cell marker; Ki67: proliferation marker. (D) Average thickness of air-liquid interface cultures treated with 40 or 50 $\mu\text{g}/\text{ml}$ nylon microfibers on the basolateral side for 4 weeks one day after seeding or upon airlifting compared to vehicle-treated control cultures. (E) Representative images of immunohistochemical stainings for proliferation and differentiation of well-developed air-liquid interface cultures treated with vehicle or 50 $\mu\text{g}/\text{ml}$ nylon microfibers on the basolateral side upon airlifting for 4 weeks. Positive staining is blue.

Figure 6. RNA-sequencing analysis of epithelial cells exposed to nylon.

(A) Estimated proportions of cell types present in Epcam⁺ cells isolated from organoids on day 7 of culture with or without 2000 (2k, equivalent to 16 $\mu\text{g}/\text{ml}$ nylon) or 5000 (5k, equivalent to 39 $\mu\text{g}/\text{ml}$ nylon) 12x31 μm nylon fibers. (B-C) Volcano plots of differentially expressed genes by epithelial cells exposed to 2000 or 5000 12x31 μm nylon fibers or not. Upregulated genes are marked in red, downregulated genes in blue. Genes were selected with thresholds of fold change >2 and $\text{FDR}<0.05$ ($n=4$). (D) Pathway analysis of genes downregulated in epithelial cells by nylon. (E) Pathway analysis of genes upregulated in epithelial cells by nylon. (F) Genes associated with airway epithelial cells. (G) Genes associated with alveolar epithelial cells. (H) Genes associated with cell proliferation. (I) Genes encoding Hox family proteins.

Figure 7. Hoxa5 is essential for airway differentiation in organoids after nylon exposure.

(A) Hoxa5 expression in murine organoids treated with/without nylon. Fluorescence images of acetylated alpha-tubulin (ACT) staining (red) and Hoxa5 expression (green). Nuclei were counterstained with DAPI (blue). (B) Representative images of immunohistochemical staining for Hoxa5 expressed by control lung organoids and lung organoids exposed to nylon for 14 days. Positive (nuclear) staining is red and nuclei are blue. (C) Representative images of murine lung organoids treated with nylon and/or Hoxa5 inhibitor LE135. (D) Quantification of number and size of murine airway or alveolar organoids treated with no or 5000 12x31 μm nylon microfibers (equivalent to 39 $\mu\text{g}/\text{ml}$) and/or LE135 (n=6). Groups were compared using a Friedman test with Dunn's correction for multiple testing. $P < 0.05$ was considered significant. (E) Representative images of human airway organoids treated with nylon and/or Hoxa5 inhibitor LE135. (F) Quantification of number and size of human airway organoids treated with nylon and/or LE135 (n=3, not statistically compared due to low n).

Figure 8. In vivo exposure of mice to nylon fibers results in long-lasting inhibition of airway epithelial differentiation as assessed by organoid formation. (A) Experimental scheme of in vivo nylon exposure. (B) Ex vivo fluorescence imaging of Nile red-labeled nylon. (C) Representative images of airway and alveolar organoids derived from epithelial cells of mice exposed to 75,000k (75k, equivalent to 298 μg nylon) or 150,000 12x31 μm nylon fibers (150k, equivalent to 597 μg nylon) or the equivalent amount of 150k leachate with or without in vitro treatment with 5 μM of Hoxa5 inhibitor LE135 (n=8). (D) Quantification of numbers of airway and alveolar organoids from all treatments. Groups of nylon-treated mice were compared using a one-way ANOVA with a Dunnett's correction for multiple testing. Organoid cultures derived from these mice and treated with LE135 were compared with a paired Student's t test. $P < 0.05$ was considered significant.

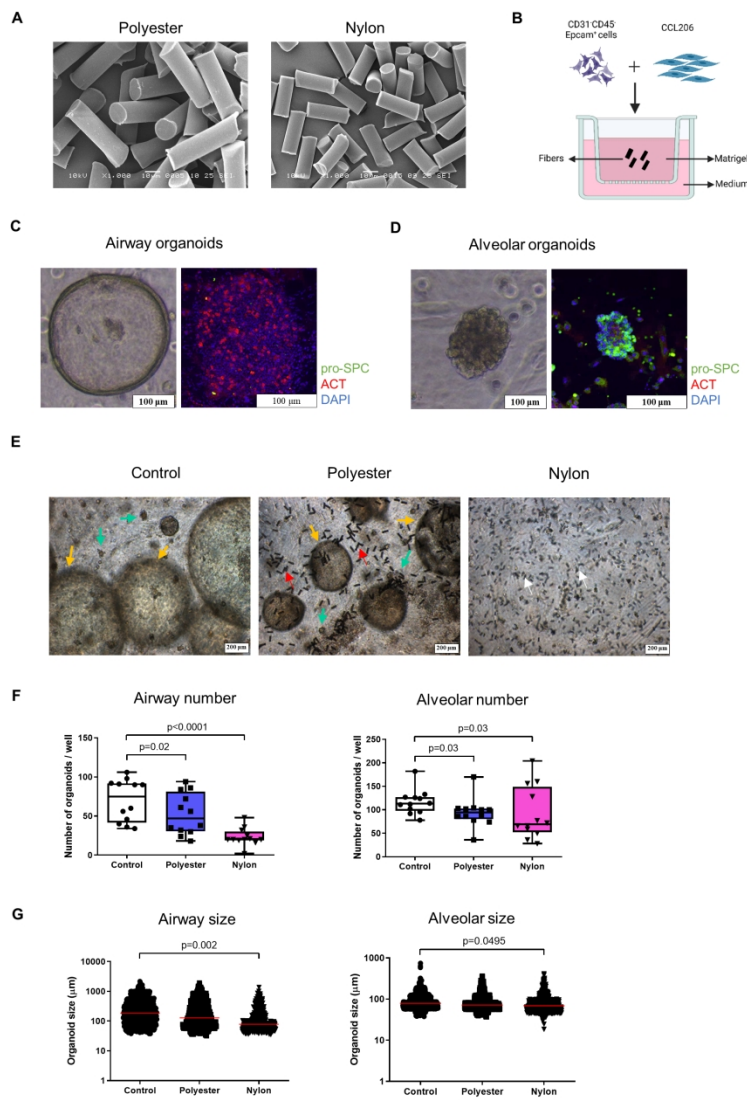


Figure 1

190x275mm (300 x 300 DPI)

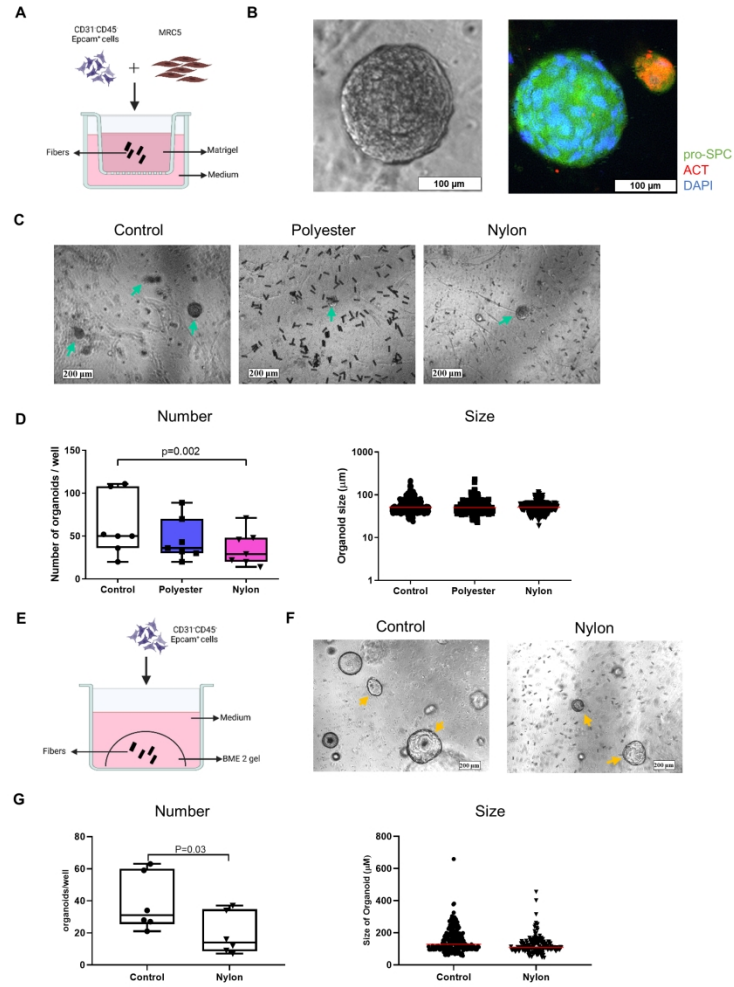


Figure 2

190x275mm (300 x 300 DPI)

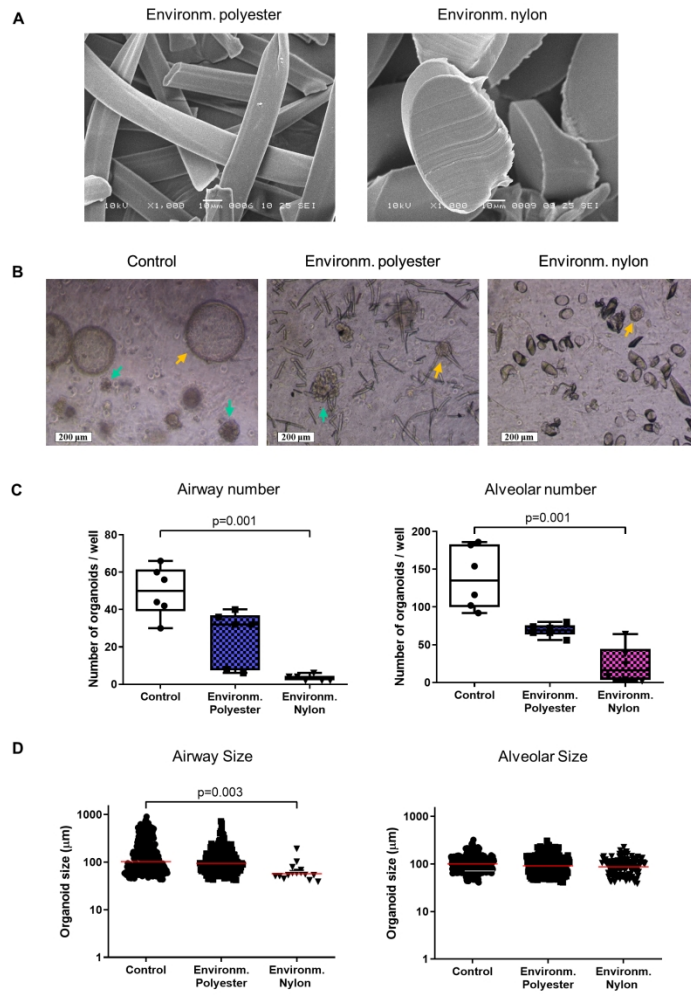


Figure 3

190x275mm (300 x 300 DPI)

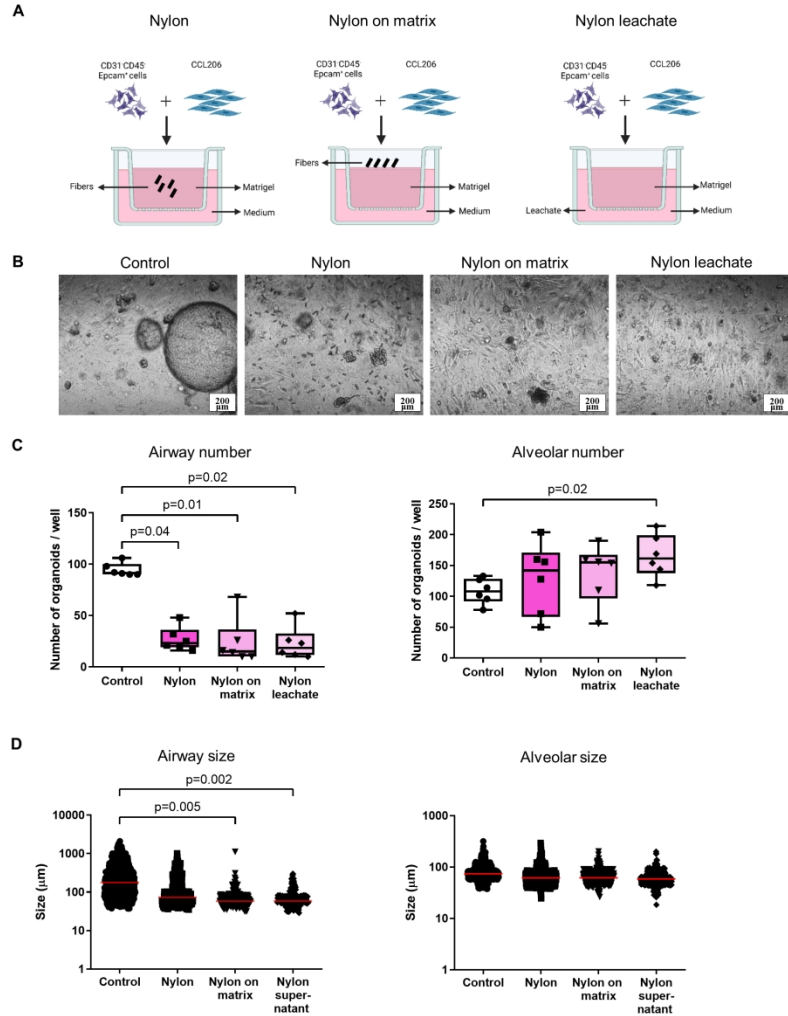


Figure 4

190x275mm (300 x 300 DPI)

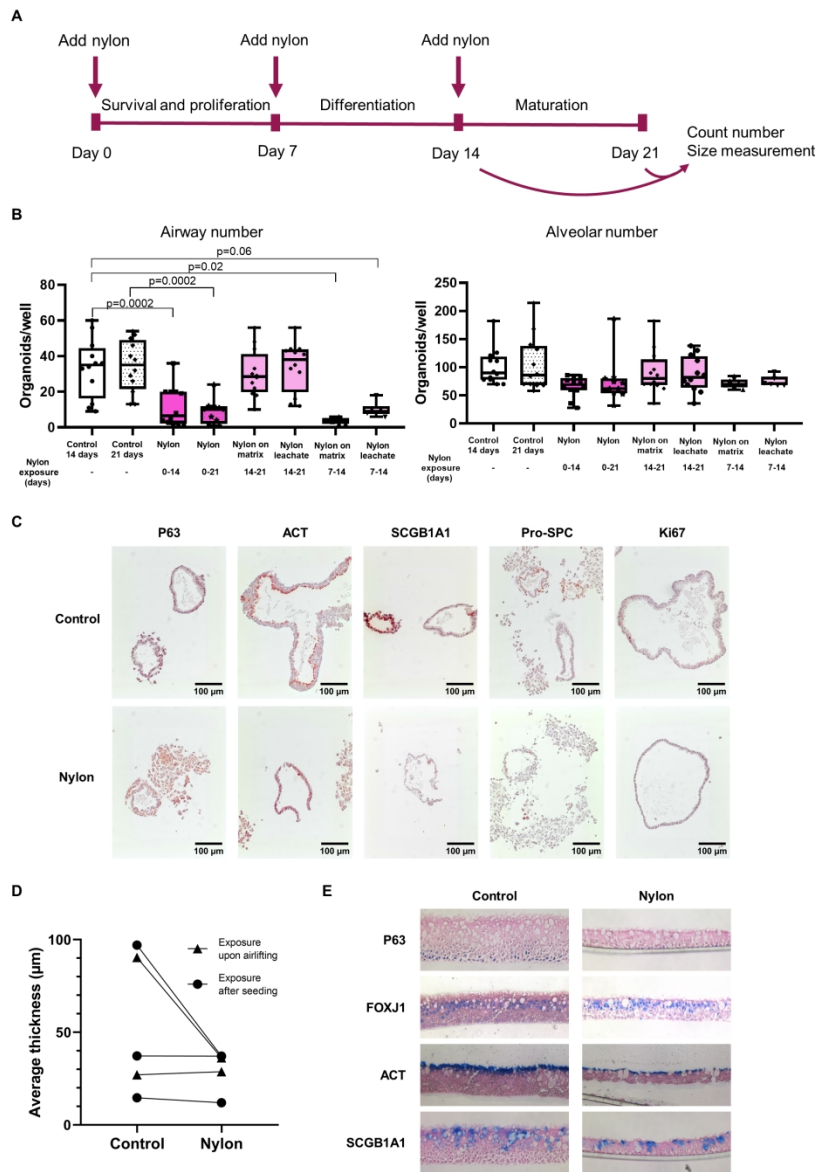


Figure 5

190x275mm (300 x 300 DPI)

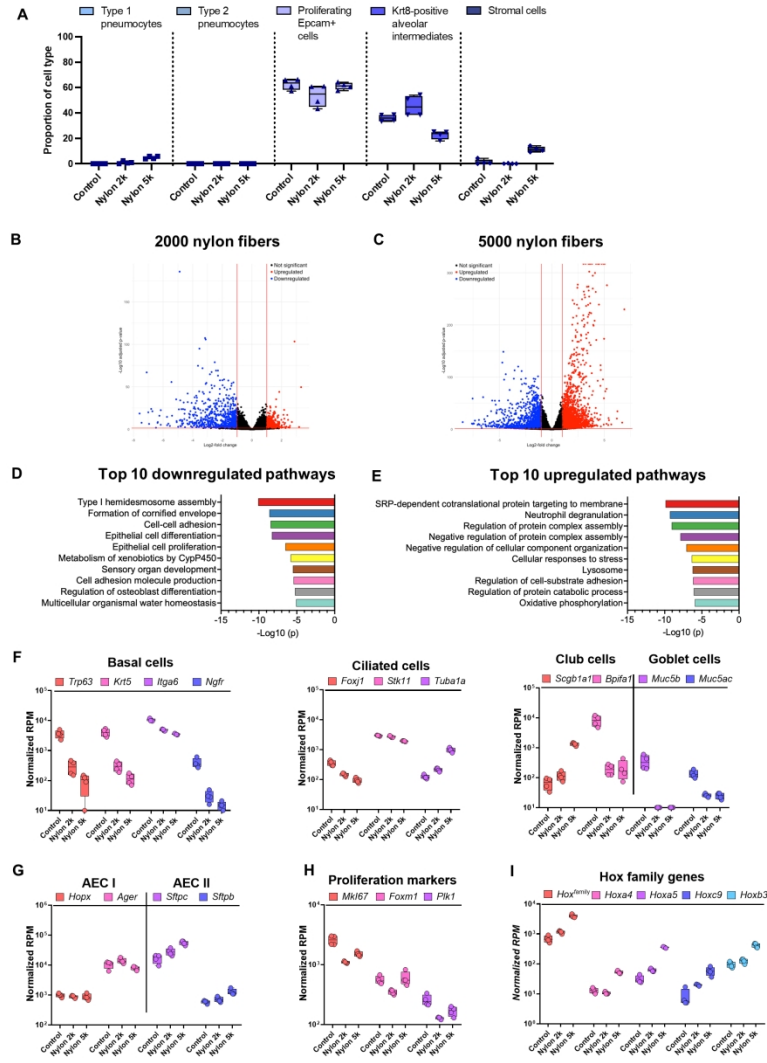


Figure 6

190x275mm (300 x 300 DPI)

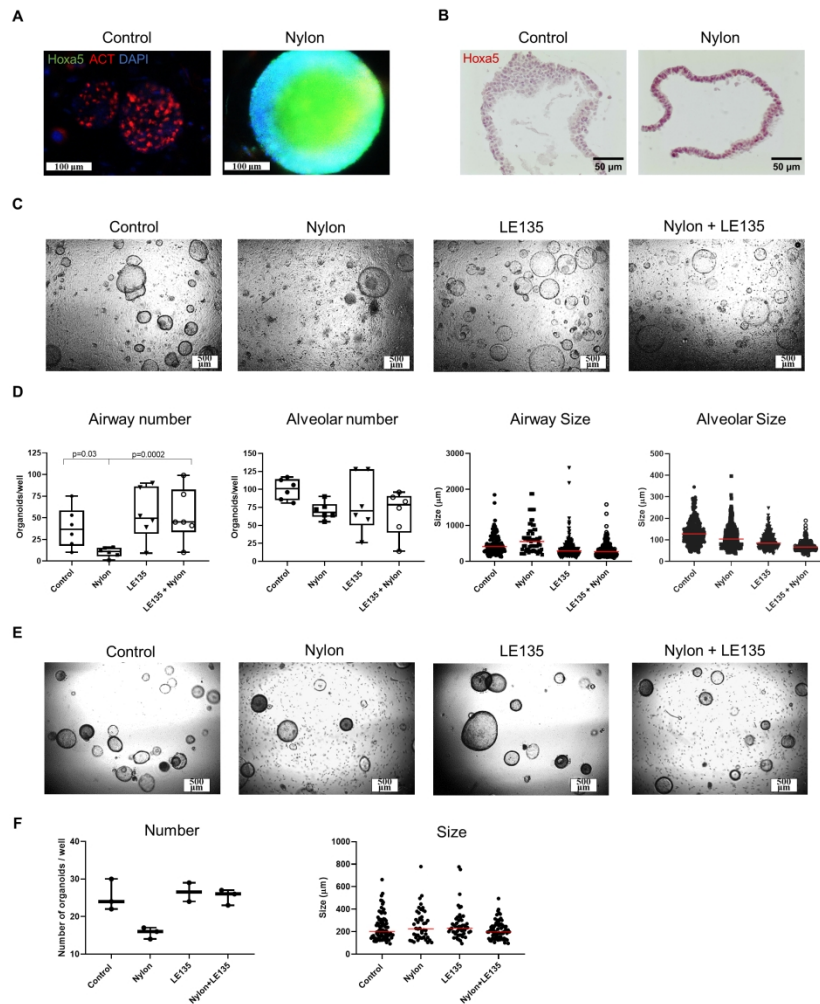


Figure 7

190x275mm (300 x 300 DPI)

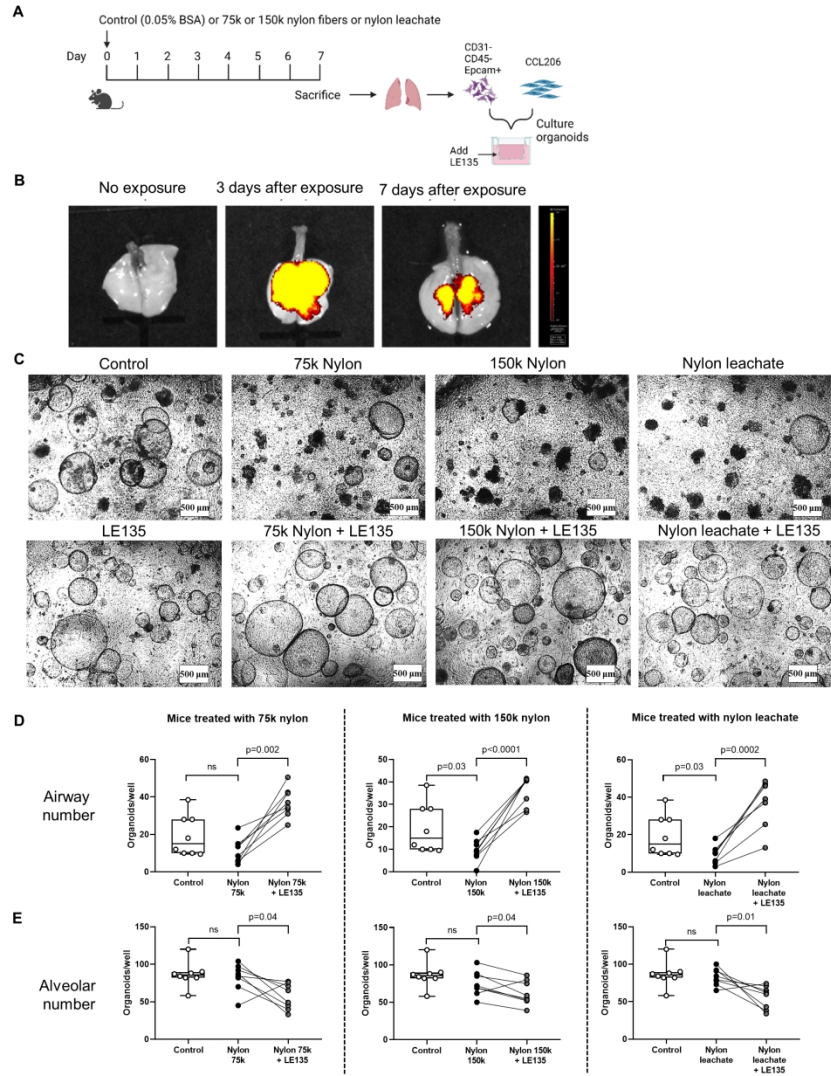


Figure 8

190x275mm (300 x 300 DPI)

Inhalable Textile Microplastic Fibers Impair Airway Epithelial Differentiation

Shanshan Song, Fransien van Dijk, Gwenda F Vasse, Qiongliang Liu, Irene F Gosselink, Ellen Weltjens, Alex HV Remels, Marina H de Jager, Sophie Bos, Chenxi Li, Tobias Stoeger, Markus Rehberg, David Kutschke, Gail van Eck, Xinhui Wu, Suzanne H Willems, Devin Boom, Ingeborg M Kooter, Diana Spierings, Rene Wardenaar, Matthew Cole, Martijn C Nawijn, Anna Salvati⁹, Reinoud Gosens, Barbro N Melgert

ONLINE DATA SUPPLEMENT

Production of microfibers and leachate

Reference microfibers and leachate

Polyethylene terephthalate (ES305710, Goodfellow, UK) or nylon 6,6 fibers (AM325705, Goodfellow, UK) with filament diameters of $14\pm 3.5\ \mu\text{m}$ and $10\pm 2.5\ \mu\text{m}$ respectively were aligned by wrapping them around a custom-made spool, coated with a thin layer of cryo compound (KP-CryoCompound, VWR International B.V., PA, USA) and frozen. Aligned fibers were cut into similar length parts ($\pm 2\ \text{cm}$) using a scalpel (Swann-Morton, UK) and moulded onto a compact block that was oriented perpendicular to the base of a cryomicrotome (Microm HM 525, Thermo Fisher Scientific, MA, USA). Microfibers were cut at lengths of $50\ \mu\text{m}$ for polyester and $30\ \mu\text{m}$ for nylon, after which the fibers were thawed, washed with 200 ml Milli-Q water through a $120\ \mu\text{m}$ filter (Merck Millipore, MA, USA) to remove miscut fibers and contaminants, collected by vacuum filtration using $8\ \mu\text{m}$ polycarbonate membrane filters (Sterlitech, WA, USA) and stored dry at -20°C .

Nylon leachate was produced by incubation of nylon reference microfibers in phosphate buffered saline (PBS) for 7 days at 37°C in the dark, followed by filtration using a $0.2\ \mu\text{m}$ syringe filter (GE Healthcare Life Sciences, UK). The leachate was stored at -20°C in dark until further use.

Environmental microfibers

Environmental polyester and nylon textile microfibers were prepared from commercially available pure fabrics. White polyester fabric was washed at 40°C in a washing machine (Samsung, South Korea) and dried in a tumble dryer (Whirlpool, MI, US). Fibers with an estimated filament diameter of $15\ \mu\text{m}$ were collected on the filter of the tumble dryer and subsequently frozen with cryo compound and sectioned into lengths of $50\ \mu\text{m}$ using a cryomicrotome. White nylon fabric (estimated filament diameter of $40\ \mu\text{m}$) was cut into small squares, stacked, frozen with cryo compound, and cut into lengths of $12\ \mu\text{m}$. All microfibers were thawed, washed with 200 ml Milli-Q water through a $120\ \mu\text{m}$ filter, collected by vacuum filtration ($8\ \mu\text{m}$ filter) and finally stored at -20°C .

Nylon microplastic particles

Nylon microplastic particles were supplied by the Momentum consortium (<https://momentummicroplastics.nl>). Briefly, polyamide 6,6 pellets (Wessling, the Netherlands) were covered by H₂O₂, and heated at 80°C with stirring at 200rpm for 3-4 hours. Polyamide pellets were then dried at 70°C and the dry polyamide was milled in a grinding beaker using a 20 mm stainless steel ball and liquid nitrogen cooling. Particles were extracted from the beaker with particle-free water. The particle solution was then sieved using several filters from 1 mm to 0.1 µm. Particles were dispersed in sterile 0.05% BSA in Milli-Q water, and stored at 4°C.

Estimation of exposure concentrations

Exposure concentrations were extrapolated from occupational exposures of around 7 mg/m³(1), a deposition efficiency of around 20% for cylindrical particles (2) , and the assumption that a factory worker would inhale around 8000 liters of air per 8-hour shift (3). Assuming a perfect distribution over a pair of lungs of around 1 kg would result in a concentration of around 11 µg/g of lung tissue *each day*, corresponding to roughly to 11 µg/ml of culture medium in organoid cultures. We therefore investigated 2000-5000 fibers per well of organoids corresponding to 16-39 µg/ml of nylon and 49-122 µg/ml polyester. For the Momentum nylon particles we tested 1, 10, and 100 µg/ml.

Characterization of microfibers

Scanning electron microscopy

Samples were prepared for scanning electron microscopy (SEM) analysis on an aluminium sample holder using adhesive carbon-coated tape. Excessive microfibers were removed using pressurized air, after which the samples were sputter-coated with 10 nm of gold. Images were obtained using a JSM-6460 microscope (Jeol, Japan) at an acceleration voltage of 10 kV.

Dimensions

Digital photomicrographs were captured at 200× magnification using a Nikon Eclipse TS100 inverted microscope coupled to a Nikon Digital Sight DS-U3 microscope camera controller (both Japan), after which microfiber diameters and lengths (median of 200) were determined using NIS-Elements AR 4.00.03 software.

Energy dispersive X-ray spectroscopy

Samples were prepared for energy dispersive X-ray (EDX) spectroscopy analysis on an aluminium sample holder using adhesive carbon coated tape. Excessive microfibers were removed using pressurized air, after which the samples were sputter coated with 10 nm of carbon. The EDX measurements were performed with a Tescan MAIA III GMH field emission scanning electron microscope (Czech Republic) equipped with a Bruker X-Flash 30 mm² silicon drift energy dispersive X-ray microanalysis detector (MA, USA).

Micro-Fourier transform infrared spectroscopy

Micro-Fourier transform infrared spectroscopy (μ FTIR) measurements were performed using a Thermo Nicolet iN10 micro-Fourier transform infrared microscope. Spectra were recorded in the wavelength range from 4000 to 675 cm⁻¹ using a spectral resolution of 8 cm⁻¹. For the transmission measurements of the polyester reference material and the polyester and nylon environmental fibers, a small amount of the microfibers was transferred onto a diamond micro compression cell where the samples were compressed. For the reflection measurements of the nylon reference material and the polyester and nylon environmental fibers, a small portion of microfibers was suspended in Milli-Q water. The suspension was subsequently filtered over a gold coated 0.8 μ m polycarbonate filter (TJ Environmental, The Netherlands). A subset of approximately 100 fibers was individually measured directly on the filter using the reflection mode of the μ -FTIR equipment.

Extraction of nylon oligomers (mono, di and trimer)

A round bottom flask containing 25.1 g cryogenically milled nylon powder (PA66, Sigma-Aldrich) and 500 ml methanol (VWR) was equipped with a reflux condenser and the

suspension was stirred overnight at 50°C. Next, the suspension was cooled to approximately 30°C and filtered over a cellulose filter (VWR) to remove the remaining powder. The solvent was removed *in vacuo* using a rotary evaporator (Büchi rotavapor R-215, Switzerland). A white solid was obtained (yield 220 mg), of which the composition was determined using liquid chromatography/mass spectrometry (LC/MS) analysis.

Isolation of nylon oligomers (mono-, di- and trimer)

A column for silica gel chromatography (\varnothing 30 mm, VWR) was charged with silica gel 60 (27 g, 0.063-0.200 mm, Merck) and dichloromethane (DCM, VWR) as eluent. The crude extract containing the mixture of oligomers (200 mg) was added on top of the silica gel column and oligomers were separated on the column using DCM:methanol as eluent (DCM:MeOH gradient: 100:0 \rightarrow 90:10 \rightarrow 80:20), which resulted in complete separation of the oligomers. The collected fractions were checked for the presence of product using LC/MS. The fractions containing pure oligomer were combined, filtered over a glass filter (VWR) and subsequently the solvent was removed *in vacuo*. The obtained solids were further dried *in vacuo*, after which the pure oligomers were obtained as white solids. The structure of the oligomers was confirmed by ^1H NMR spectroscopy.

^1H Nuclear magnetic resonance of oligomers

The chemical structure of the oligomers was confirmed by ^1H NMR spectroscopy (Bruker Avance 400 spectrometer). The oligomers were dissolved in ~ 0.5 ml $\text{CD}_3\text{OD}:\text{CDCl}_3$ (1:1) (Sigma-Aldrich). The spectra were recorded at 24 °C, and internally referenced to the residual solvent resonance (CD_3OD : ^1H δ 3.31).

Nylon monomer, yield = 77 mg. ^1H NMR (400.1 MHz, $\text{CD}_3\text{OD}/\text{CDCl}_3$ 50:50, 297 K) δ = 7.56 (br. m, 2H; NHCO), 3.22 (m, 4H, NHCH_2), 2.19 (m, 4H, COCH_2), 1.63 (m, 4H, COCH_2CH_2), 1.54 (m, 4H, NHCH_2CH_2), 1.32 (m, 4H, $\text{NH}(\text{CH}_2)_2\text{CH}_2$).

Nylon dimer, yield = 74 mg. ^1H NMR (400.1 MHz, $\text{CD}_3\text{OD}/\text{CDCl}_3$ 50:50, 297 K) δ = 7.68 (br. m, 4H; NHCO), 3.15 (t, 8H, NHCH_2), 2.18 (m, 8H, COCH_2), 1.60 (m, 8H, COCH_2CH_2), 1.47 (m, 8H, NHCH_2CH_2), 1.31 (m, 8H, $\text{NH}(\text{CH}_2)_2\text{CH}_2$).

Nylon trimer, yield = 16 mg. ^1H NMR (400.1 MHz, $\text{CD}_3\text{OD}/\text{CDCl}_3$ 50:50, 297 K) δ = 7.74 (br. m, 6H; NHCO), 3.14 (t, 12H, NHCH_2), 2.18 (m, 12H, COCH_2), 1.60 (m, 12H, COCH_2CH_2), 1.48 (m, 12H, NHCH_2CH_2), 1.32 (m, 12H, $\text{NH}(\text{CH}_2)_2\text{CH}_2$).

Liquid chromatography/mass spectrometry

Qualitative analysis of nylon leachate and oligomers

Qualitative analysis of nylon oligomers was performed with an Agilent 1260 series high-performance liquid chromatographer (CA, USA) equipped with a 100 x 2 mm, 3 μm Gemini NX-C18 110 Å LC Column (Phenomenex, Utrecht, The Netherlands), coupled with an Agilent 6410 triple quadrupole LC/MS with electron spray ionization (ESI) in positive SCAN mode. In addition, the LC/MS analysis of the nylon leachate was performed with the Agilent 1260 liquid chromatographer coupled to an Agilent 6460 triple quadrupole LC/MS with Jetstream ESI in positive SCAN mode. A sample volume of 5 μl was injected with a column temperature of 60 °C and a flow rate of 200 $\mu\text{l min}^{-1}$. The sample was eluted with a gradient of Milli-Q water (containing 5 mM ammonium formate with 0.0025% formic acid (both Sigma-Aldrich), eluent A) and methanol (containing 5 mM ammonium formate with 0.0025% formic acid, eluent B) with a flow rate of 0.5 ml min^{-1} . Eluent B was increased from 10% to 90% in 10 minutes and maintained for 3 minutes. After this, eluent B was decreased to 10% in 0.1 minute and maintained for 1.9 minutes to complete the cycle of 15 minutes. Mass spectrometry was performed with a gas temperature of 350 °C and a flow rate of 10 l min^{-1} . Stealth gas temperature (for Agilent 6460) was set at 400 °C with a flow rate of 12 l min^{-1} . The capillary voltage was set at 4000 V.

Direct injection of nylon leachate

An injection volume of 10 μl diluted nylon leachate was directly injected into an Agilent 6410 triple quadrupole MS system with ESI in positive SCAN mode. The conditions were as follows: gas temperature 350 °C, flow rate 10 l min^{-1} , mobile phase 50:50 ratio of 80:20 acetonitrile (VWR):Milli-Q water with 5 mM ammonium formate and 10:90 acetonitrile: Milli-Q water with 5 mM ammonium formate, scan range 50–1000 Da, capillary voltage 3500 V.

Nile red labelled nylon fibers

Nylon fibers were transferred with 2.5 ml of Nile Red solution (500 $\mu\text{g ml}^{-1}$, technical grade, N3013, SigmaAldrich) into 5 ml Eppendorf tubes. Tubes were shortly vortexed and then incubated for 10 minutes at room temperature. Nylon fibers were collected by vacuum filtration (8 μm filter) and rinsed with acetone to remove surplus dye and then washed with several times of 200 ml Milli-Q water. Fluorescent nylon fibers were kept in the dark at 4 °C.

Ethics

Animal experiments

The experimental protocol for the use of mice for epithelial cell isolations was approved by the institutional animal care and use committee of the University of Groningen (IVD 15303-01-004)) and for *in vivo* application of fibers and subsequent cell isolation by the Government of Upper Bavaria (ROB-55.2Vet-2532.Vet_02-19-150). All experiments were performed according to strict governmental and international guidelines on animal experimentation. Male and female C57BL/6 mice (8-14 weeks) were bred at the Central Animal Facility of the University Medical Center Groningen (UMCG) or were purchased from Charles River (Sulzfeld, Germany). Animals received ad libitum normal diet with a 12 h light/dark cycle.

Human lung tissue

For organoid cultures, histologically normal lung tissue was anonymously donated by individuals with COPD or without COPD undergoing surgery for lung cancer or lung transplantation for COPD and not objecting to the use of their tissue. Sections of lung tissue of each patient were stained with a standard haematoxylin and eosin staining and checked for abnormalities by a lung pathologist before tissue was used. COPD patients included ex and current smoking individuals with GOLD stage I-IV disease. Lung organoid cultures were derived from tissue of patients with varying severity of COPD or not (n=7, GOLD I=1, GOLD II=2, GOLD IV=3, non-COPD=1) and airway organoids were exclusively derived from lung tissue of patients with severe COPD (n=7, GOLD IV). Subjects with other lung diseases such as asthma, cystic fibrosis, or interstitial lung diseases were excluded. The study protocol

was consistent with the Research Code of the University Medical Center Groningen (UMCG) and Dutch national ethical and professional guidelines (www.federa.org) and approved by the medical ethical committee of the UMCG. Patient characteristics for Epcam+ cells used in human lung organoid experiments and human airway organoid experiments are listed in Table 1a and Table 1b respectively.

Primary bronchial epithelial cells for air-liquid interface culture were isolated from lung tissue derived from the Maastricht Pathology Tissue Collection (MPTC). Guidelines were followed as outlined in 'Human Tissue and Medical Research: Code of conduct for responsible use' (2011) (www.federa.org). Ethics approval for the use of human tissue was granted by both the scientific board of the MPTC (code MPTC2010-019) and the local Medical Ethics Committee (code 2017-0087). Tissues were anonymously coded during tissue collection, storage and subsequent use. Primary bronchial epithelial cells were isolated from resected lung tissue of two patients with no history of chronic lung diseases who underwent surgery for solitary pulmonary nodules. Alternatively, primary bronchial epithelial cells were isolated from leftover, de-identified tracheal-bronchial tissue from healthy donor lungs at the University Medical Center Groningen (UMCG). The study protocol was compliant with the Research Code of the University Medical Center Groningen and Dutch national ethical and professional guidelines (www.federa.org). Available patient characteristics are described in Table 1c.

Table 1a. Demographics and clinical characteristics of patients whose lung tissue was used for isolation of Epcam+ cells to grow lung organoids .

Type	Sex, F/M	Age, yr	Smoking status	Pack-years	FEV1/FVC	COPD GOLD Stage
Non-COPD	0/1	68	ES	15	73	NA
COPD	2/4	62 (52-65)	CS/ES (1), CS (1), ES (4)	25 (15-58)	46 (21-58)	I (1), II (2), IV (3)

F/M: female or male; ES: exsmoking; CS: current smoking; FEV1/FVC: ratio between forced expiratory volume in 1 s (FEV1) and forced vital capacity (FVC); NA: not applicable. Values are median (interquartile range).

Table 1b. Demographics and clinical characteristics of patients whose lung tissue was used for isolation of Epcam+ cells to grow airway organoids .

Type	Sex, F/M	Age, yr	Smoking status	Pack-years	FEV1/FVC	COPD GOLD Stage
COPD	4/3	58 (54-61)	ES (7)	25 (14-32)	28 (21-30)	IV (7)

F/M: female or male; ES: exsmoking; CS: current smoking; FEV1/FVC: ratio between forced expiratory volume in 1 s (FEV1) and forced vital capacity (FVC); NA: not applicable. Values are median (interquartile range).

Table 1c. Available demographics and clinical characteristics of patients whose lung tissue was used for primary bronchial epithelial cell isolation and subsequent air-liquid interface culture.

Donor nr.	Center	Type	Sex, F/M	Age, yr	Smoking status	FEV1/FVC
1	MUMC	Non-COPD	M	73	ES	79
2	MUMC	Non-COPD	M	72	ES	70
3	UMCG	Healthy	Unknown	Unknown	Unknown	NA
4	UMCG	Healthy	Unknown	Unknown	Unknown	NA
5	UMCG	Healthy	Unknown	Unknown	Unknown	NA

F/M: female or male; ES: exsmoking; FEV1/FVC: ratio between forced expiratory volume in 1 s (FEV1) and forced vital capacity (FVC); NA: not applicable.

Exposure of mice to nylon microfibers or leachate

Mice were exposed with either 50 µl vehicle (0.05% BSA in PBS) for control groups, 50 µl 75k (equivalent to 298 µg) or 150k nylon fibers (equivalent to 597 µg) nylon fiber

suspension, or equivalent amounts of 150k nylon leachate by intratracheal instillation as described before (4). Briefly, the mice were anesthetized by intraperitoneal injection with a combination of medetomidine (0.5 mg/kg bodyweight), midazolam (5 mg/kg bodyweight), and fentanyl (0.05 mg/kg bodyweight) and the trachea was intubated with a 20G cannula (Braun, Melsungen) for instillation. Mouse lung tissues were collected 7 days after exposure. Each experimental group contained eight mice.

***Ex vivo* whole lung imaging**

To determine the distribution of Nile red fibers in murine lung tissue, an IVIS system (Lumina II, Caliper/PerkinElmer, USA) was used for whole organ imaging of isolated lungs. In short, whole lungs were placed on a platform located in the center of the IVIS chamber and imaged (535/DsRed – excitation/emission). The fluorescence/white light images were acquired with Living Imaging 4.0 software (Caliper, Hopkinton, USA) to determine the fluorescence intensity and the 2D projected geometric area of the lung.

Cell cultures

Mouse lung fibroblasts (CCL-206, ATCC, Wesel, Germany) or human lung fibroblasts (MRC5, ATCC, CCL-171) were cultured in 1:1 DMEM (Gibco, MD, USA) and Ham's F12 (Lonza, Switzerland) or Ham's F12 respectively, both supplemented with 10% heat inactivated fetal bovine serum (FBS, GE Healthcare Life Sciences), 100 U/ml penicillin-streptomycin, 2 mM L-glutamine and 2.5 µg/ml amphotericin B (all Gibco). Fibroblasts were cultured at 37°C under 5% CO₂ and humidified conditions. For use in organoid cultures, near-confluent cells were proliferation-inactivated by incubation with 10 µg/ml mitomycin C (Sigma-Aldrich, MO, USA) in cell culture medium for 2 hours, after which they were washed in PBS, and left in normal medium for at least 1 hour before trypsinizing and counting.

To produce R-Spondin 1 or Noggin-conditioned media, HEK293T Noggin hFc cells or HEK293 R-Spondin 1 hFc cells were cultured in DMEM (Gibco, MD, USA) with additional 100 U/ml penicillin-streptomycin and 10% FBS as described previously (5, 6).

Cell viability assay

10,000 murine Epcam+ cells were seeded per well in 96-well plates. After cell attachment, the cells were treated with 39 µg/mL nylon fibers, 39 µg/mL nylon leachate or 0.05% BSA as vehicle control. Cells treated with 10% DMSO were included as a positive control. After 72h, MTS CellTiter 96 AQueous One Solution Reagent (Promega, Madison, WI, USA) was added to the cell culture medium and incubated for 120 min at 37 °C in a humidified atmosphere containing 5% CO₂. The absorbance was determined at a wavelength of 490 nm using a Synergy H1 plate reader (BioTek, Winooski, VT, USA).

Lung epithelial cell isolation

Mouse lung epithelial cell isolation

Epithelial cells were isolated from lungs of mice using antibody-coupled magnetic beads (microbeads) as described before. In short, mice were sacrificed under anaesthesia, after which the lungs were flushed with 0.9% NaCl and instilled with 75 caseinolytic units/1.5 ml dispase (Corning, NY, USA). After 45 minutes of incubation at room temperature, the lobes (excluding trachea and extrapulmonary airways) were homogenized in DMEM containing 100 U/ml penicillin-streptomycin and 40 µg/ml DNase1 (PanReac AppliChem, Germany), washed in DMEM (containing penicillin, streptomycin and DNase1), and the digested tissue was passed through a 100 µm cell strainer. The suspension was incubated for 20 minutes at 4°C with anti-CD31 and anti-CD45 microbeads in MACS buffer and magnetically sorted using LS columns. The CD31-/CD45- flow-through was incubated for 20 minutes at 4°C with anti-CD326 (EpCAM) microbeads in MACS buffer, after which purified epithelial lung cells were obtained by positive selection using LS columns. CD326-positive epithelial cells were resuspended in CCL206 fibroblast medium, counted and seeded into growth factor-reduced Matrigel matrix (Corning) immediately after isolation with equal numbers of CCL206 fibroblasts, as described below. All materials were purchased at Miltenyi Biotec (Germany) unless stated otherwise.

Human lung epithelial cell isolation

Human lung epithelial cells were isolated from lung tissue specimens obtained from patients. Peripheral lung tissue was minced and dissociated in DMEM-containing enzymes (Multi Tissue Dissociation Kit) at 37°C using a gentleMACS Octo Dissociator. The cell suspension was filtered (70 µm and 35 µm strainer, respectively) prior to 20-minute incubation at 4°C with anti-CD31 and anti-CD45 microbeads in MACS buffer. The CD31⁻/CD45⁻ fraction was obtained by negative selection using an AutoMACS. Epithelial cells were then isolated by positive selection after 20-minute incubation at 4°C with anti-CD326 (EpCAM) microbeads in MACS buffer. Human EpCAM⁺ cells were resuspended in 1:1 DMEM and Ham's F12, supplemented with 10% heat inactivated FBS, 100 U/ml penicillin-streptomycin, 2 mM L-glutamine and 2.5 µg/ml amphotericin B, counted and seeded into growth factor-reduced Matrigel matrix (Corning) immediately after isolation with equal numbers of MRC5 fibroblasts. All materials were purchased at Miltenyi Biotec unless stated otherwise.

Lung organoid cultures

Lung organoids were grown as previously described with minor modifications (7, 8). For mouse lung organoids, 10,000 EpCAM⁺ cells and 10,000 CCL206 fibroblasts were seeded, and for human lung organoids, 5,000 EpCAM⁺ cells and 5,000 MRC5 fibroblasts were seeded in 100 µl growth factor-reduced Matrigel matrix (Corning) diluted 1:1 in DMEM:Ham's F-12 1:1 containing 10% FBS, 100 U/ml penicillin-streptomycin, 2 mM L-glutamine and 2.5 µg/ml amphotericin B into transwell 24-well cell culture plate inserts (Corning). Organoids were cultured in DMEM:Ham's F-12 1:1 supplemented with 5% FBS, 100 U/ml penicillin-streptomycin, 2 mM L-glutamine, 2.5 µg/ml amphotericin B, 4 ml/l insulin-transferrin-selenium (Gibco), 25 µg/l recombinant mouse (Sigma-Aldrich) or human epithelial growth factor (EGF, Gibco) and 700 µl/l bovine pituitary extract (Sigma-Aldrich). 10 µM Y-27632 (Axon Medchem, the Netherlands) was only added to the medium during first 48 hours. All organoid cultures were maintained for 14 to 21 days at 37 °C under 5% CO₂ and humidified conditions. Medium with or without 5 µM LE135 (TOCRIS #2021) was refreshed every two days.

A titration curve for polyester or nylon microfibers was made with 2000, 3000, 4000 or 5000 fibers per well corresponding to approximately 49, 73, 98 and 122 $\mu\text{g}/\text{ml}$ of polyester fibers or 16, 23, 31, and 39 $\mu\text{g}/\text{ml}$ of nylon fibers. For all other experiments, 5000 polyester or nylon reference fibers (equivalent to 122 $\mu\text{g}/\text{ml}$ of polyester or 39 $\mu\text{g}/\text{ml}$ of nylon) or environmental microfibers (equivalent to 189 $\mu\text{g}/\text{ml}$ polyester or 531 $\mu\text{g}/\text{ml}$ nylon) were used per condition.

Fibers were in direct contact with developing organoids during 14 days by mixing them with Matrigel and cells prior to seeding in the insert, except for those experiments studying effects of leaching nylon components. In those cases, 5000 polyester or nylon fibers were added on top of the organoids, thereby excluding physical contact between the microfibers and the developing organoids, or equivalent amounts of fiber leachate were added to the medium during 14 days of organoid culture.

For testing the effects of nylon oligomers, concentrations between 27 ng/ml and 54 $\mu\text{g}/\text{ml}$ were used: the latter concentration being twice as high as the used fiber concentrations (5000 fibers per condition). Oligomers were isolated and characterized as described before in the supplementary materials and methods. For testing the effects of other possible nylon leachates 0.001mM-10mM PEG600 (Merck # 1546467), 1-100 ng/ml Benzophenone-3, or 2 ng/ml-2000ng/ml BPA (Sigma #133027) were added to media.

For testing the effects of nylon and its leachate on airway epithelial differentiation, 5000 nylon fibers were mixed with Matrigel-cell suspension and cultured for 14 or 21 days, or 5000 nylon fibers were added on top of the organoids, or equivalent amounts of fiber leachate were added to the medium during 14, or 7-14 or 14-21 days of organoid culture.

The number of organoids was counted manually after 14 or 21 days of culturing using a light microscope. For mouse organoids, a distinction was made between airway and alveolar organoids, whereas for human organoids only one organoid phenotype was distinguished. The diameter of the organoids was measured using a light microscope (Nikon, Eclipse Ti), only including organoids larger than 50 μm in diameter.

Human airway organoid culture (6)

20,000 human primary Epcam+ cells were resuspended with 5000 nylon fibers in Cultrex growth factor-reduced Basement Membrane Extract (BME2, R&D 3533-010-02). Droplets of 50 μ l BME2-cell mixture were added on pre-warmed 24-well suspension culture plates (Greiner-M9312) at 37°C for 30 min. After solidification, 500 μ l of advanced BMEM/F12 medium (Invitrogen) containing human FGF7 (25ng/ml, Peprotech), human FGF10 (100 ng/ml, Peprotech), 10% R-Spondin 1 conditioned medium, 10% Noggin-conditioned medium, ROCK inhibitor Y27632 (5 μ M, Sigma), A83-01 (500 nM, Tocris), SB202190 (500 nM, Sigma), nicotinamide (5 mM, Sigma), B27 supplement (Gibco), n-acetylcysteine (1.25 mM, Sigma), HEPES (10 mM, Invitrogen), penicillin/streptomycin (100 U/ml, Invitrogen), primocin (50 mg/ml, Invitrogen) was added to each well. Medium with or without 2.5 μ M LE135 was changed every 4 days. After 21 days, the total number of organoids was counted and the size of organoids was measured manually. The diameter of the organoids was measured using a light microscope (Nikon, Eclipse Ti), only including organoids larger than 100 μ m in diameter.

Primary bronchial epithelial cell isolation and air-liquid interface culture

Primary bronchial epithelial cells were isolated by the primary lung culture (PLUC) facility at MUMC+ as previously described (9, 10). In the UMCG, primary bronchial epithelial cells were acquired from tracheal-bronchial tissue through protease digestion. The tracheal-bronchial tissue was rinsed twice in Hanks' Balanced Salt Solution (HBSS, Lonza, Basel, Switzerland) supplemented with 1% penicillin (10,000 U/ml)/streptomycin (10,000 μ g/ml) (P/S, Gibco). Any non-tracheal-bronchial tissue was then eliminated, and the remaining tissue was cut into small fragments. These fragments were placed in dissociation buffer, consisting of airway epithelial basal medium (AEBM, Promocell) supplemented with 1% P/S, 1.5 mg/ml protease type XIV (Sigma-Aldrich, Darmstadt, Germany) and 0.2 μ l/ml DNase I (Roche, Basel, Switzerland), and left to incubate overnight at 4°C. The following day, the dissociation buffer was collected from the tissue, along with two additional HBSS washes. All the cells were collected by centrifugation for 5 minutes at 500g and counted using a Bürker-Türk counting chamber. The cells were then cryopreserved until further use.

Primary bronchial epithelial cells (5×10^5 cells, passage 1) were thawed, seeded and expanded in pre-coated flasks (coating: $10 \mu\text{g/ml}$ BSA (Sigma, A8806-5g), $10 \mu\text{g/ml}$ human fibronectin (Sigma, F1056-1MG), $30 \mu\text{g/ml}$ PureCol Type I Bovine Collagen Solution (Advanced BioMatrix, 5005-B)) in airway epithelial growth medium (AEGM, Promocell) supplemented with 1% P/S (UMCG) or expansion medium including pneumacultTM-Ex basal medium (StemCell Technologies, #5008), 1X pneumacultTM-Ex supplement (StemCell Technologies, #5019), $0.096 \mu\text{g/ml}$ hydrocortisone (StemCell Technologies, #7925) and 100 U/ml penicillin/ $100 \mu\text{g/ml}$ streptomycin (Gibco, 15140122) following the manufacturer's protocol of pneumacultTM-Ex medium (MUMC). Every 2 days, primary bronchial epithelial cells were washed with HBSS (Gibco, 14175-129) followed by refreshment of the culture medium. When cells reached 80% confluency they were seeded (passage 3) at a density of 75,000 cells per pre-coated 0.33 cm^2 ThinCert cell culture insert (Greiner) in AEGM (UMCG) or 40,000 cells per pre-coated 1.10 cm^2 polyethylene terephthalate inserts (CellQART, 9310412) in the pneumacultTM-Ex medium (MUMC). Cells were grown submerged until 95% confluency, at which point primary bronchial epithelial cells were airlifted by removing apical medium and replacing the basolateral medium with ALI medium. The ALI medium contained DMEM (25 mM HEPES and 4.5 g/L glucose, Lonza) with AEBM in a 1:1 ratio supplemented with an AEGM growth supplement mix (Promocell), 1% P/S, $1.5 \mu\text{g/ml}$ BSA and 15 ng/ml fresh retinoic acid (Sigma) (UMCG) or pneumacultTM-ALI basal medium (StemCell Technologies, #5001), 1X pneumacultTM-ALI supplement, 1X PneumacultTM-ALI maintenance supplement, $4 \mu\text{g/ml}$ heparin solution (StemCell Technologies, #7980), $0.48 \mu\text{g/ml}$ hydrocortisone (StemCell Technologies, #7925) and 100 U/ml penicillin/ $100 \mu\text{g/ml}$ streptomycin (Gibco, 15140122) following the manufacturer's protocol of pneumacultTM-ALI maintenance medium (MUMC). Every 2 days both apical and basolateral sides were washed with HBSS (Gibco) to remove excess mucus. Cultures were maintained at ALI for 26-32 days at 37°C and 5% CO_2 and continuously exposed to vehicle (0.05% BSA in PBS) or nylon microfibers from the basolateral side directly after cells attached to the inserts (day 1 after seeding, $40 \mu\text{g/ml}$, donor 3-5, UMCG) or from the moment of airlifting ($50 \mu\text{g/ml}$, donor 1-2, MUMC). Transepithelial electrical resistance was monitored at an approximately 7-day interval in ALI cultures using an epithelial tissue voltohmmeter (World Precision

Instruments). TEER ($\Omega\cdot\text{cm}^2$) was corrected for the surface area of the inserts and background measurements of an empty coated insert without cells.

RNA isolation, cDNA synthesis and real-time quantitative PCR

26 days after airlifting, total RNA was extracted from ALI cultures by lysis in TRIzol reagent (Invitrogen) and subsequent processing according to the manufacturer's instructions. RNA quality and quantity was measured using a NanoDrop 1000 spectrophotometer (Thermo Scientific). 750 ng RNA was reverse transcribed into cDNA using M-MLV reverse transcriptase according to the manufacturer's instructions (Promega). Real-time quantitative PCR was performed with 10 ng cDNA/reaction, 1 μM forward and reverse primers for the genes of interest (Table 2) and FastStart Universal SYBR Green Master (ROX, Roche) using a QuantStudio 7 Flex System. Gene expression levels were normalized to the average expression of housekeeping genes cyclophilin A and RPL13A by using the $2^{-\text{ddCt}}$ method.

Table 2. List and sequences of primers used in this manuscript

Gene	Forward primer	Reverse primer
Cyclophilin A	CATCTGCACTGCCAAGACTGA	TTCATGCCTTCTTTCACTTTGC
RPL13A	CCTGGAGGAGAAGAGGAAAGAGA	TTGAGGACCTCTGTGTATTTGTCAA
Scgb1a1	TTCAGCGTGTCATCGAAACCC	ACAGTGAGCTTTGGGCTATTTTT
KRT5	GGAGTTGGACCAGTCAACATC	TGGAGTAGTAGCTTCCACTGC
TP63	CCCGTTTCGTCAGAACACAC	CATAAGTCTCACGGCCCCTC
FOXJ1	TCGTATGCCACGCTCATCTG	CTTGATAGATGGCCGACAGGG

Immunofluorescence organoid staining

Organoid cultures in Matrigel were washed with PBS, fixed in ice-cold 1:1 acetone and methanol (both Biosolve Chimie, France) for 15 minutes at -20°C and washed again with PBS after which nonspecific antibody-binding was blocked for 2 hours with 5% bovine serum albumin (BSA, Sigma-Aldrich). Organoids were incubated overnight at 4°C with the

primary antibodies (mouse anti-acetylated α -tubulin (Santa Cruz, TX, USA) and rabbit anti-prosurfactant protein C (Merck, Germany)) both diluted 1:200 in 0.1% BSA and 0.1% Triton (Sigma-Aldrich) in PBS. Next, after extensive but gentle washing with PBS, organoids were incubated with the appropriate Alexa-conjugated secondary antibody for 2 hours at room temperature (Alexa Fluor 488 donkey anti rabbit IgG and Alexa Fluor 568 donkey anti mouse IgG, both Thermo Fisher Scientific) diluted 1:200 in 0.1% BSA and 0.1% Triton in PBS. Organoid cultures were washed with PBS, excised using a scalpel, mounted on glass slides (Knittel, Germany) using mounting medium containing DAPI (Sigma-Aldrich) and covered with a cover glass (VWR). Digital photomicrographs were captured at 200 \times magnification using a DM4000b fluorescence microscope and LAS V4.3 software (both Leica, Germany).

Organoid immunohistochemistry

To harvest organoids from the Matrigel, the basolateral supernatant was removed and 100 μ L warm (37 $^{\circ}$ C) dispase (Corning) was added apically. After 45 minutes, the Matrigel was dissolved and MACS rinsing solution was added to stop the reaction and allow transfer to an Eppendorf tube. Pipet tips were cut and coated with 3% BSA in PBS to prevent disruption of organoids and sticking of organoids to the pipet tip. The tubes were centrifuged at low speed (200g) for 3 minutes and the pelleted organoids were subsequently resuspended in 4% PFA for fixation at room temperature for 10 minutes, followed by two PBS washes. The organoids were then resuspended in warm HistoGel (65 $^{\circ}$ C, Thermo Fisher) and left to solidify as a droplet for 30 minutes, before placing them in cassettes in 70% ethanol. The HistoGel droplet with organoids was then embedded in paraffin according to the standard protocol and cut into 4 μ m sections.

Following deparaffinization, antigen retrieval was performed by heating the sections in citric acid (10 mM, pH 6.0) in a pressure cooker. After three PBS washes, sections were incubated in 0.5% Triton in PBS for 10 minutes, followed by three more PBS washes. Sections were subsequently blocked in 5% BSA 5% normal mouse serum (NMS, Invitrogen) in PBS or 5% BSA in PBS (ACT only) for 15 minutes, before adding the primary antibody (ACT, HoxA5, Ki67, P63, Pro-SPC or Scgb1a1, Table 3) in 2% BSA 5% NMS in PBS or 2% BSA in PBS (ACT only). After 1 hour incubation and three PBS washes, endogenous peroxidases

were blocked with 0.3% H₂O₂ in methanol or 3% H₂O₂ in methanol (ACT only) for 20 minutes. Sections were then washed twice in demi water and three times in PBS before adding the HRP-linked secondary antibody (Table 3) in the same diluents for 1 hour. After three PBS washes, staining was visualized using ImmPACT NovaRED HRP Substrate Kit (Vector laboratories) according to the manufacturer's instructions and counterstained with Mayer's Hematoxylin (Sigma). Sections were subsequently dehydrated, mounted in non-aqueous mounting medium and imaged using an Olympus BX40 microscope. Representative pictures were selected for both nylon exposed and vehicle control.

ALI immunohistochemistry

30-32 days after airlifting, ALI cultures were washed 3 times in PBS and fixed by adding 4% PFA to both the apical and basolateral side of the inserts. After 1.5 hours, the inserts were washed in PBS and stored in 70% ethanol until further processing. Inserts were embedded in paraffin and 4 µm paraffin sections were stained using immunohistochemistry. For the Scgb1a1 staining, antigen retrieval was performed in citric acid (10mM; pH6) and all sections were blocked with 5% BSA (Sigma, A4503-10G) for 30 minutes at room temperature. Primary antibodies (FoxJ1, ACT, p63 and Scgb1a1) were incubated overnight at 4 °C at the indicated dilutions (Table 3). Biotinylated secondary antibodies were incubated at room temperature for 1 hour (Table 3). The alkaline phosphatase kit (Vectastain AK-5000) in combination with the Vector blue AP substrate kit (Vector SK5300) were used to visualize the presence of the intended antigens. Sections were mounted with Vectamount (non-aqueous, H-5000-60) and imaged using a Leica DM4 B Upright Microscope.

Table 3. List of antibodies and dilutions used in this manuscript

Protein	Product nr.	Company	Sample	Dilution
Acetylated alpha-tubulin (ACT)	SC-23950	Santa Cruz	mouse organoids	1:2000
Acetylated alpha-tubulin (ACT)	T7451	Sigma	ALI	1:20,000
FoxJ1	14-9965-82	Invitrogen	ALI	1:200

HoxA5	PA5-101638	Invitrogen	mouse organoids	1:300
Ki67	AB15580	Abcam	mouse organoids	1:200
P63	AB124762	Abcam	ALI/mouse organoids	1:200
Pro-SPC	AB90716	Abcam	mouse organoids	1:800
Scgb1a1	07 632	Millipore	mouse organoids	1:2000
Scgb1a1	HM2178	Sanbio	ALI	1:200
Goat-a-Rabbit IgG/HRP	4049-05	Southern Biotech	mouse organoids	1:300
Rabbit-a-Mouse IgG/HRP	6175-05	Southern Biotech	mouse organoids	1:300
Rabbit-a-Mouse IgG/Biotin	E0413	DAKO	ALI	1:200
Swine-a-Rabbit IgG/Biotin	E0353	DAKO	ALI	1:200

Isolation of epithelial cells and fibroblasts from organoid cultures

200,000 murine EpCAM+ primary cells and 200,000 CCL206 fibroblasts (n=4 independent isolations) were seeded in 1 ml Matrigel diluted 1:1 in DMEM containing 10% FBS in 6-well plates (Greiner Bio-One, The Netherlands). 12,000 or 30,000 nylon microfibers (equivalent to 2k and 5k fibers in smaller wells) were mixed with Matrigel and cells prior to seeding. Murine organoid culture medium was maintained on top and refreshed every two days. After 7 days, organoid cultures were digested with 50 caseinolytic units/ml dispase for 30 minutes at 37°C, transferred to 15 ml tubes, washed with MACS BSA stock solution and autoMACS rinsing solution (both Miltenyi), and digested further with trypsin (VWR) diluted 1:5 in PBS for 5 minutes at 37°C. The cell suspension was then incubated for 20 minutes at 4°C with anti-EpCAM microbeads in MACS buffer, after which the suspension was passed through LS columns. Both the EpCAM+ (epithelial cells) and EpCAM- (fibroblasts) cell fractions were used for RNA isolation and subsequent sequencing.

Library preparation and RNA sequencing

Total RNA was isolated from EpCAM+ and EPCAM- cell fractions using a Maxwell[®] LEV simply RNA Cells/Tissue kit (Promega, WI, USA) according to manufacturer's instructions. RNA concentrations were determined using a NanoDrop One spectrophotometer (Thermo Fisher Scientific). Total RNA (300 ng) was used for library preparation. Paired-end sequencing was performed using a NextSeq 500 machine (Illumina; mate 1 up to 74 cycles and mate 2 up to 9 cycles). Mate 1 contained the first STL (stochastic labeling) barcode, followed by the first bases of the sequenced fragments, and mate 2 only contained the second STL barcode. The generated data were subsequently demultiplexed using sample-specific barcodes and changed into fastq files using bcl2fastq (Illumina; version 1.8.4). The quality of the data was assessed using FastQC. The STL barcodes of the first mate were separated from the sequenced fragments using an in-house Perl script. Low quality bases and parts of adapter sequences were removed with Cutadapt (version 1.12; settings: q=15, O=5, e=0.1, m=36). Sequenced poly A tails were removed as well, by using a poly T sequence as adapter sequence (T (100); reverse complement after sequencing). Reads shorter than 36 bases were discarded. The trimmed fragment sequences were subsequently aligned to all known murine cDNA sequences using HISAT2 (version 2.1.0; settings: k=1000, --norc). The number of reported alignments, k, was given a high number in order to not miss any alignment results (some genes have up to 62 transcripts). Reads were only mapped to the forward strand (directional sequencing). Fragment sequences that mapped to multiple genes were removed (unknown origin). When fragments mapped to multiple transcripts from the same gene all but one were given a non-primary alignment flag by HISAT2 (flag 256). These flags were removed (subtraction of 256) by the same Perl script in order to be able to use the Bash-based shell script (dqRNASeq; see below) that is provided by Bioo Scientific (Perkin Elmer, MA, USA). Fragments that mapped to multiple transcripts from the same gene were considered unique and were counted for each of the transcripts. The number of unique fragments (or read pairs) was determined for each transcript using the script provided by Bioo Scientific (dqRNASeq; settings: s=8, q=0, m=1). Counts that were used for further analysis were based on a unique combination of start and stop positions and barcodes (USS + STL). The RNAseq data have been deposited to the Gene Expression Omnibus GEO with dataset identifier GSE238065.

Data analyses

For RNA sequencing data, the principal component analyses were performed in R using the R package DESeq2 (version 1.26.0) to visualize the overall effect of experimental covariates as well as batch effects (function: plotPCA). Differential gene expression analyses (treated vs. nontreated) were performed with the same R package (default settings; negative binomial GLM fitting and Wald statistics; design= \sim mouse+condition), following standard normalization procedures. Genes with differential expression >2 (nylon-treated versus nontreated fibroblasts or epithelial cells) and a false discovery rate smaller than 0.05 (FDR) were considered differentially expressed in that specific cell type. Volcano plots were made in R studio using ggplot2 and clustering heat maps were made using BioJupies. Pathway analysis was done using Metascape. Cellular deconvolution of bulk RNA sequencing data from Epcam+ cells was done using MuSIC (11) with a single cell sequencing dataset from Angelidis *et al.* (12) for freshly isolated epithelial cells and a dataset from Choi *et al.* (13) for epithelial cells isolated from 7-day organoid cultures.

Statistics

Statistical analyses were either performed in GraphPad Prism 9.0 or in R studio (R Studio 2022.02.2+485 "Prairie Trillium" Release). For data $n < 8$ nonparametric testing was used to compare groups, whereas for $n > 8$ parametric testing was used if data were normally distributed as assessed from QQ plots. For comparison of multiple groups, a Kruskal wallis or Friedman test was used for nonpaired or paired nonparametric data respectively with Dunn's correction for multiple testing or a paired/unpaired one-way ANOVA for parametric data with Sidak's correction for multiple testing. Differences in organoid size between groups were tested by using the average size of the organoids per independent replicate. Data are presented as median \pm range and p-values < 0.05 were considered significant.

References

1. Wright SL, Kelly FJ. Plastic and Human Health: A Micro Issue? *Environ Sci Technol* 2017;51:6634–6647.
2. Mohammad S. Islam¹, Md. Mizanur Rahman, Puchanee Larpruenrudee, Akbar Arsalanloo, Hamidreza Mortazavy Beni, Md. Ariful Islam, YuanTong Gu and ES. How Microplastics are Transported and Deposited in Realistic Upper Airways? *Phys Fluids* 2023;0–26.at <<https://doi-org.proxy-ub.rug.nl/10.1063/5.0150703>>.
3. Pleil JD, Ariel Geer Wallace M, Davis MD, Matty CM. The physics of human breathing: flow, timing, volume, and pressure parameters for normal, on-demand, and ventilator respiration. *J Breath Res* 2021;15:.
4. Ganguly K, Upadhyay S, Irmeler M, Takenaka S, Pukelsheim K, Beckers J, Hamelmann E, Schulz H, Stoeger T. Pathway focused protein profiling indicates differential function for IL-1B, -18 and VEGF during initiation and resolution of lung inflammation evoked by carbon nanoparticle exposure in mice. *Part Fibre Toxicol* 2009;6:31.
5. Vonk AM, van Mourik P, Ramalho AS, Silva IAL, Statia M, Kruisselbrink E, Suen SWF, Dekkers JF, Vlegaar FP, Houwen RHJ, Mullenders J, Boj SF, Vries R, Amaral MD, de Boeck K, van der Ent CK, Beekman JM. Protocol for Application, Standardization and Validation of the Forskolin-Induced Swelling Assay in Cystic Fibrosis Human Colon Organoids. *STAR Protoc* 2020;1:100019.
6. Sachs N, Papaspyropoulos A, Zomer-van Ommen DD, Heo I, Böttinger L, Klay D, Weeber F, Huelsz-Prince G, Iakobachvili N, Amatngalim GD, Ligt J, Hoeck A, Proost N, Viveen MC, Lyubimova A, Teeven L, Derakhshan S, Korving J, Begthel H, Dekkers JF, Kumawat K, Ramos E, Oosterhout MF, Offerhaus GJ, Wiener DJ, Olimpio EP, Dijkstra KK, Smit EF, Linden M, *et al.* Long-term expanding human airway organoids for disease modeling. *EMBO J* 2019;38:1–20.
7. Ng-Blichfeldt JP, de Jong T, Kortekaas RK, Wu X, Lindner M, Guryev V, Hiemstra PS, Stolk J, Königshoff M, Gosens R. Tgf- β activation impairs fibroblast ability to support

adult lung epithelial progenitor cell organoid formation. *Am J Physiol - Lung Cell Mol Physiol* 2019;317:L14–L28.

8. Wu X, Bos IST, Conlon TM, Ansari M, Verschut V, van der Koog L, Verkleij LA, D'Ambrosi A, Matveyenko A, Schiller HB, Königshoff M, Schmidt M, Kistemaker LEM, Yildirim AÖ, Gosens R. A transcriptomics-guided drug target discovery strategy identifies receptor ligands for lung regeneration. *Sci Adv* 2022;8:1–15.
9. van Wetering S, Zuyderduyn S, Ninaber DK, van Sterkenburg MAJA, Rabe KF, Hiemstra PS. Epithelial differentiation is a determinant in the production of eotaxin-2 and -3 by bronchial epithelial cells in response to IL-4 and IL-13. *Mol Immunol* 2007;44:803–811.
10. Van Wetering S, Van Der Linden AC, Van Sterkenburg MAJA, De Boer WI, Kuijpers ALA, Schalkwijk J, Hiemstra PS. Regulation of SLPI and elafin release from bronchial epithelial cells by neutrophil defensins. *Am J Physiol - Lung Cell Mol Physiol* 2000;278:51–58.
11. Wang X, Park J, Susztak K, Zhang NR, Li M. Bulk tissue cell type deconvolution with multi-subject single-cell expression reference. *Nat Commun* 2019;10:.
12. Angelidis I, Simon LM, Fernandez IE, Strunz M, Mayr CH, Greiffo FR, Tsitsiridis G, Ansari M, Graf E, Strom TM, Nagendran M, Desai T, Eickelberg O, Mann M, Theis FJ, Schiller HB. An atlas of the aging lung mapped by single cell transcriptomics and deep tissue proteomics. *Nat Commun* 2019;10:1–17.
13. Choi J, Park J-E, Tsagkogeorga G, Yanagita M, Koo B-K, Han N, Lee J-H. Inflammatory Signals Induce AT2 Cell-Derived Damage-Associated Transient Progenitors that Mediate Alveolar Regeneration. *Cell Stem Cell* 2020;27:366-382.e7.

Supplementary tables and figures

Table E1. Size characteristics of polyester and nylon microfibers.

	Microfiber size Diameter x length (μm)	
	Polyester	Nylon
25% percentile	14x50	11x29
Median	15x52	12x31
75% percentile	15x53	12x32
Minimum	13x22	9x24
Maximum	18x64	14x74

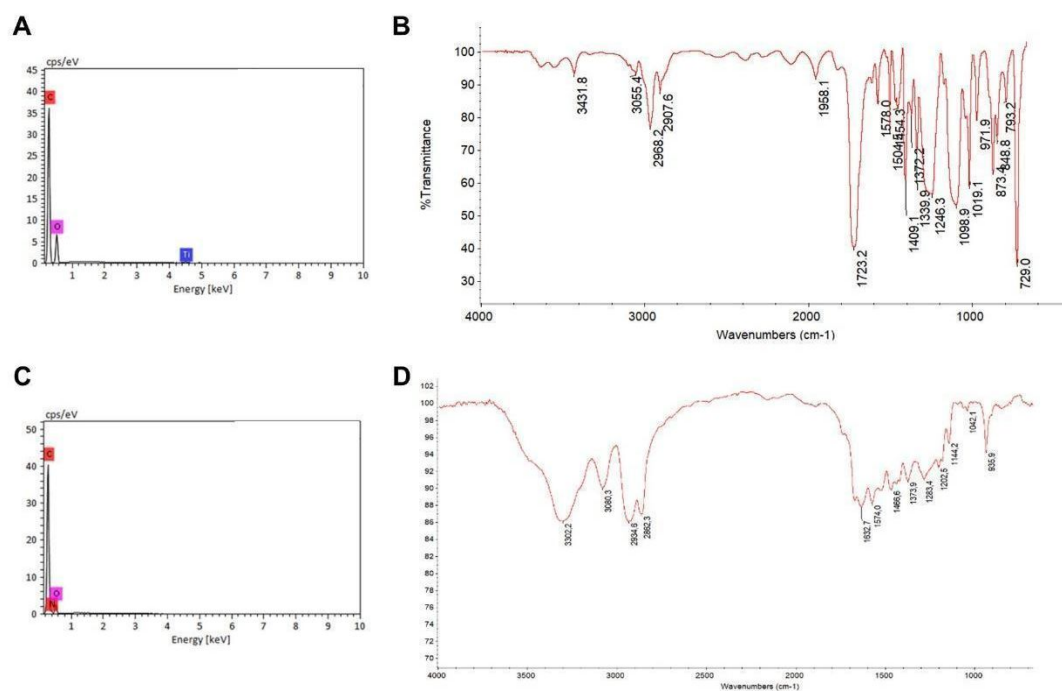


Figure E1: Characterization of nylon and polyester microfibrers using energy dispersive X-ray and infrared spectroscopy.

(A) EDX spectrum of polyester, confirming the presence of carbon (C) and oxygen (O), and additionally revealing the presence of titanium (Ti), which can be ascribed to small TiO₂ pigment particles used as filler material in these fibers. (B) μ FTIR spectrum of polyester with characteristic absorbance peaks (2968 cm⁻¹, C-H stretch; 1723 cm⁻¹, C=O stretch; 1246 cm⁻¹, C-O stretch aromatic ester; 729 cm⁻¹, benzene derivative). (C) EDX spectrum of nylon, confirming the presence of carbon (C), nitrogen (N) and oxygen (O). (D) μ FTIR spectrum of nylon with characteristic nylon absorbance peaks (3302 cm⁻¹, N-H stretch; 2934 cm⁻¹, C-H stretch; 1632 cm⁻¹, C=O stretch sec. amide; 1202 cm⁻¹, C-N bend).

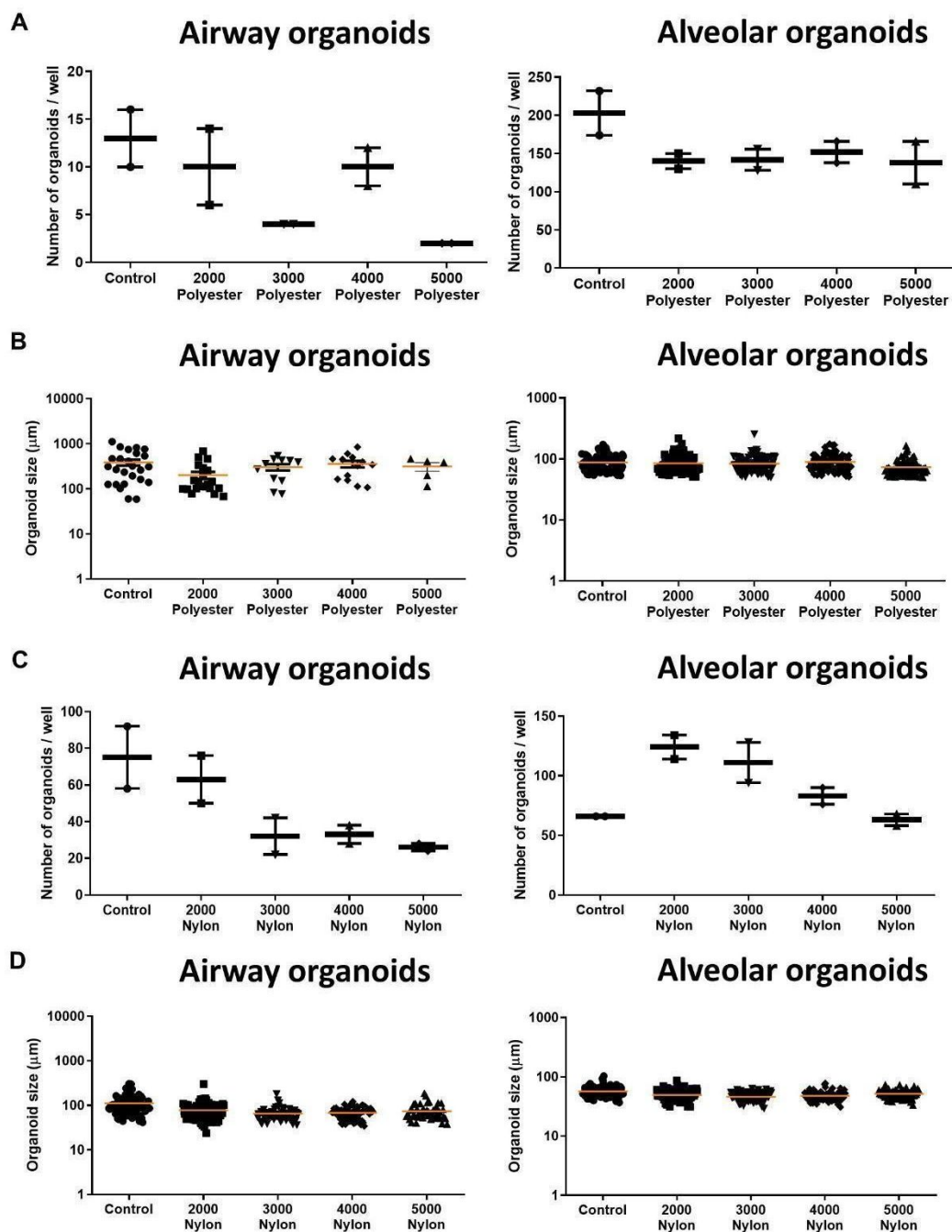


Figure E2: Determination of the optimal microfiber dose for subsequent *in vitro* testing of polyester and nylon microfibers, using 2000, 3000, 4000 and 5000 microfibers per condition.

(A) The number of airway and alveolar organoids for organoids exposed to $15 \times 52 \mu\text{m}$ polyester fibers (n=2 independent experiments). (B) The size of airway and alveolar organoids exposed to $15 \times 52 \mu\text{m}$ polyester fibers (n=2 independent experiments). (C) The number of airway and alveolar organoids exposed to $12 \times 31 \mu\text{m}$ nylon fibers (n=2 independent experiments). (D) The size of airway and alveolar organoids exposed to

26

12x31 μm nylon fibers (n=2 independent experiments). 2000, 3000, 4000 or 5000 fibers per well corresponded to approximately 49, 73, 98 and 122 $\mu\text{g}/\text{ml}$ of polyester fibers or 16, 23, 31, and 39 $\mu\text{g}/\text{ml}$ of nylon fibers.

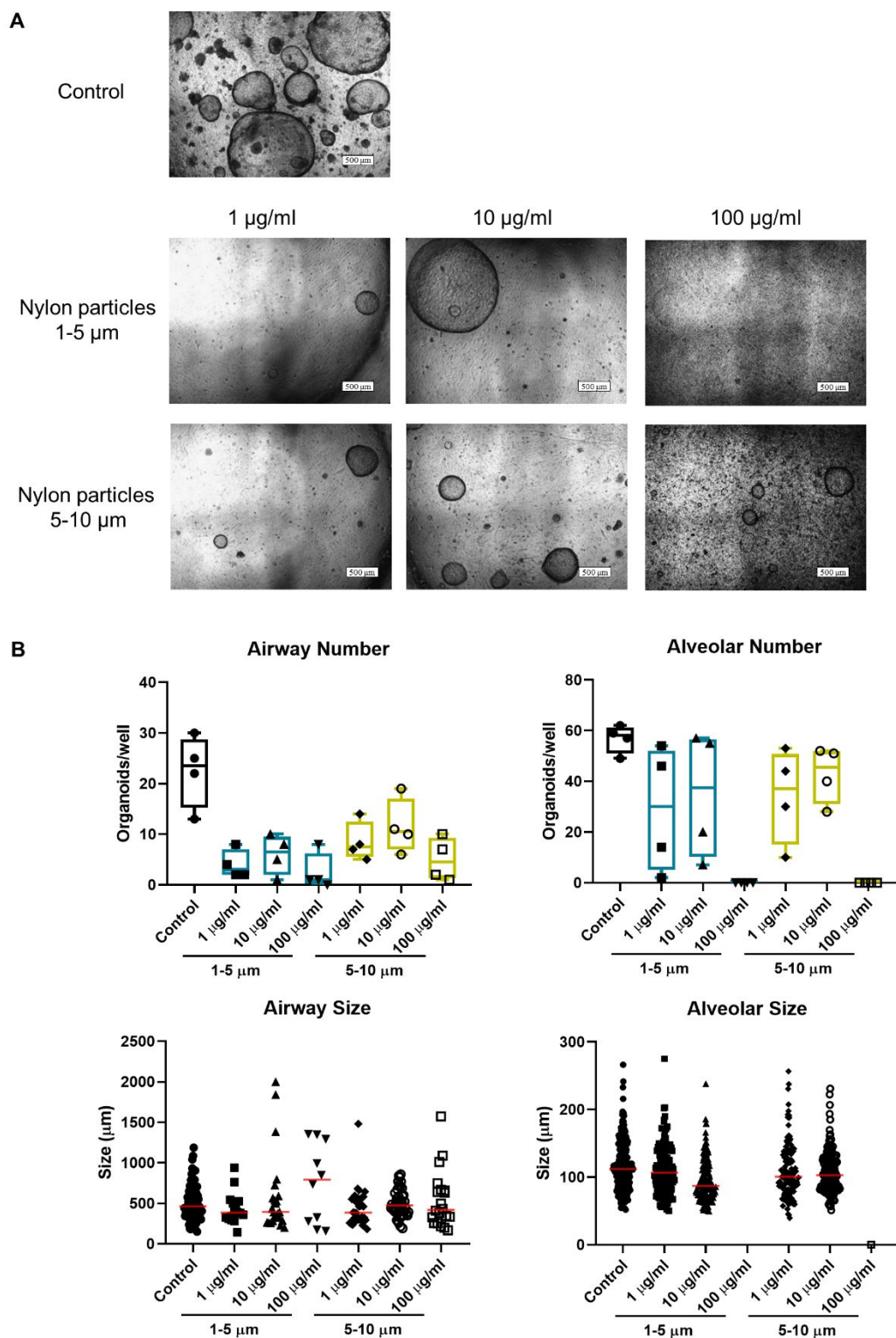


Figure E3. Effects of nylon particles on growth of murine lung organoids.

(A) Representative light microscopy images of the different treatment conditions. (B) Quantification of the numbers and the sizes of airway and alveolar lung organoids

exposed to different concentrations of irregularly shaped nylon particles of 1-5 μm or 5-10 μm from the Momentum consortium (n=4 independent experiments).

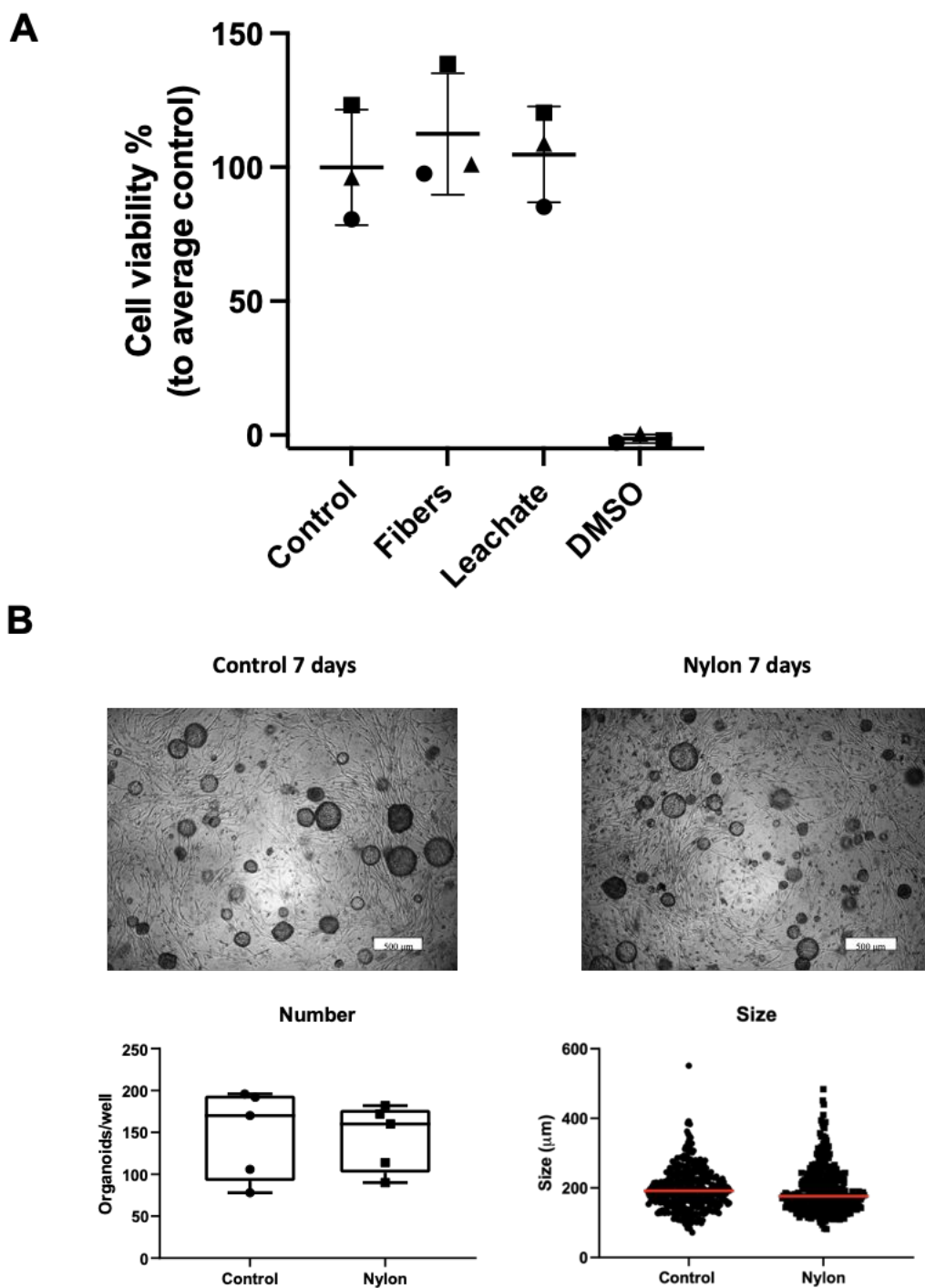


Figure E4. Nylon microfibers have no effects on proliferation of Epcam+ cells isolated from murine lung tissue.

(A) Viability of Epcam+ cells isolated from murine lung tissue as assessed by MTS assay at 72 h after exposure to 39 $\mu\text{g}/\text{mL}$ 12x31 μm nylon fibers, 39 $\mu\text{g}/\text{mL}$ nylon leachate or 0.05% BSA as vehicle control. DMSO-treated cells were included as a positive control. Each different symbol represents cells of a different mouse (n=3 mice). (B) Representative

light microscopy images of murine lung organoids after 7 days of treatment with 12x31 μm nylon fibers (5000 fibers/well) or not and quantification of their numbers and sizes.

Table E2. Size characteristics of polyester and nylon environmental microfibers.

	Microfiber size Diameter x length (μm)	
	Environmental polyester	Environmental nylon
25% percentile	15x54	46x15
Median	17x63	57x20
75% percentile	18x85	73x27
Minimum	8x30	17x8
Maximum	24x269	296x66

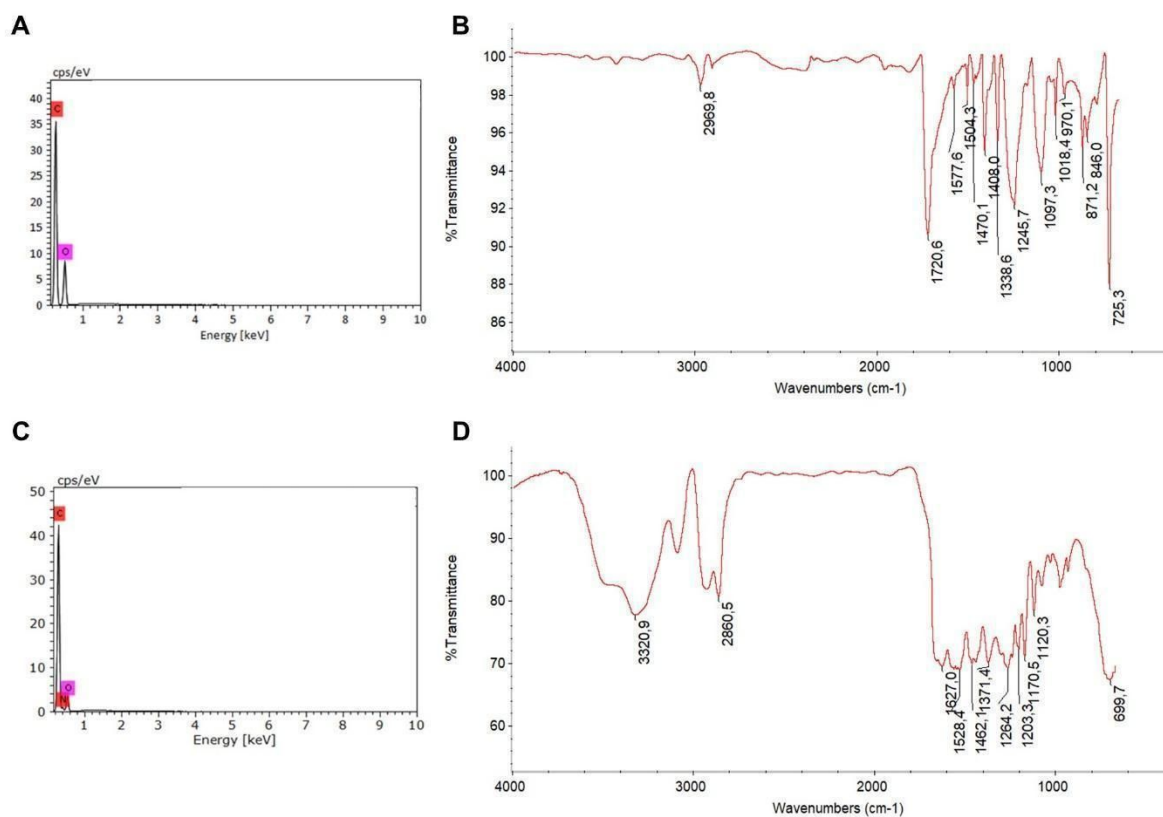


Figure E5. Characterization of the environmental microfibers using energy dispersive X-ray - and infrared spectroscopy. EDX and μ -FTIR spectra of (A and B) polyester and (C and D) nylon microfibers.

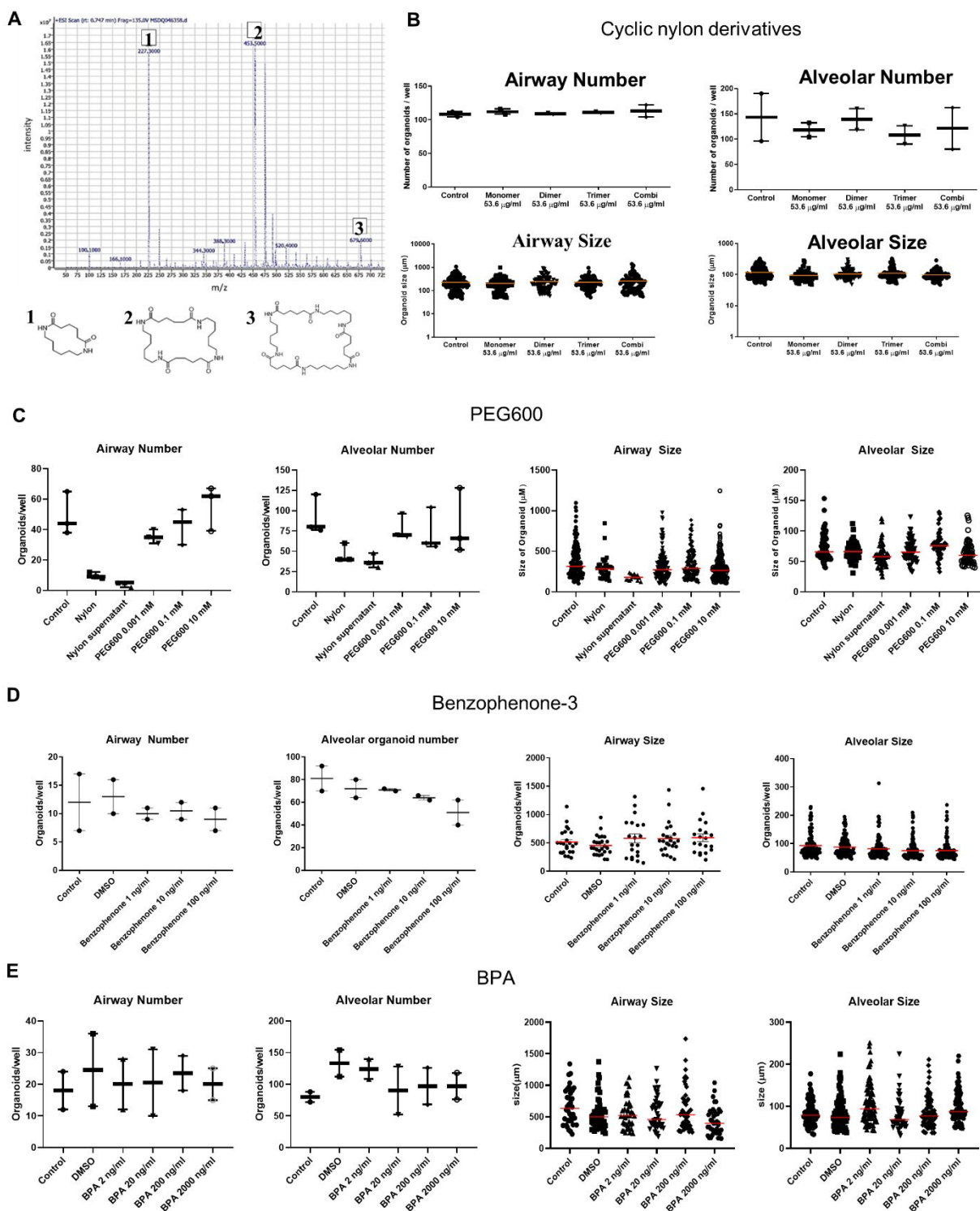


Figure E6. Characterization of components leaching from nylon microfibers and their effect on organoid growth.

(A) Mass spectrometry spectrum of nylon leachate, revealing high amounts of cyclic nylon mono-, di- and trimers, as well as other smaller peaks. The effects of (B) cyclic nylon

mono-, di- and trimers, (C) PEG600, (D) Benzophenone-3 and (E) BPA on the number of airway and alveolar organoids and their sizes (n=2 or 3 independent experiments).

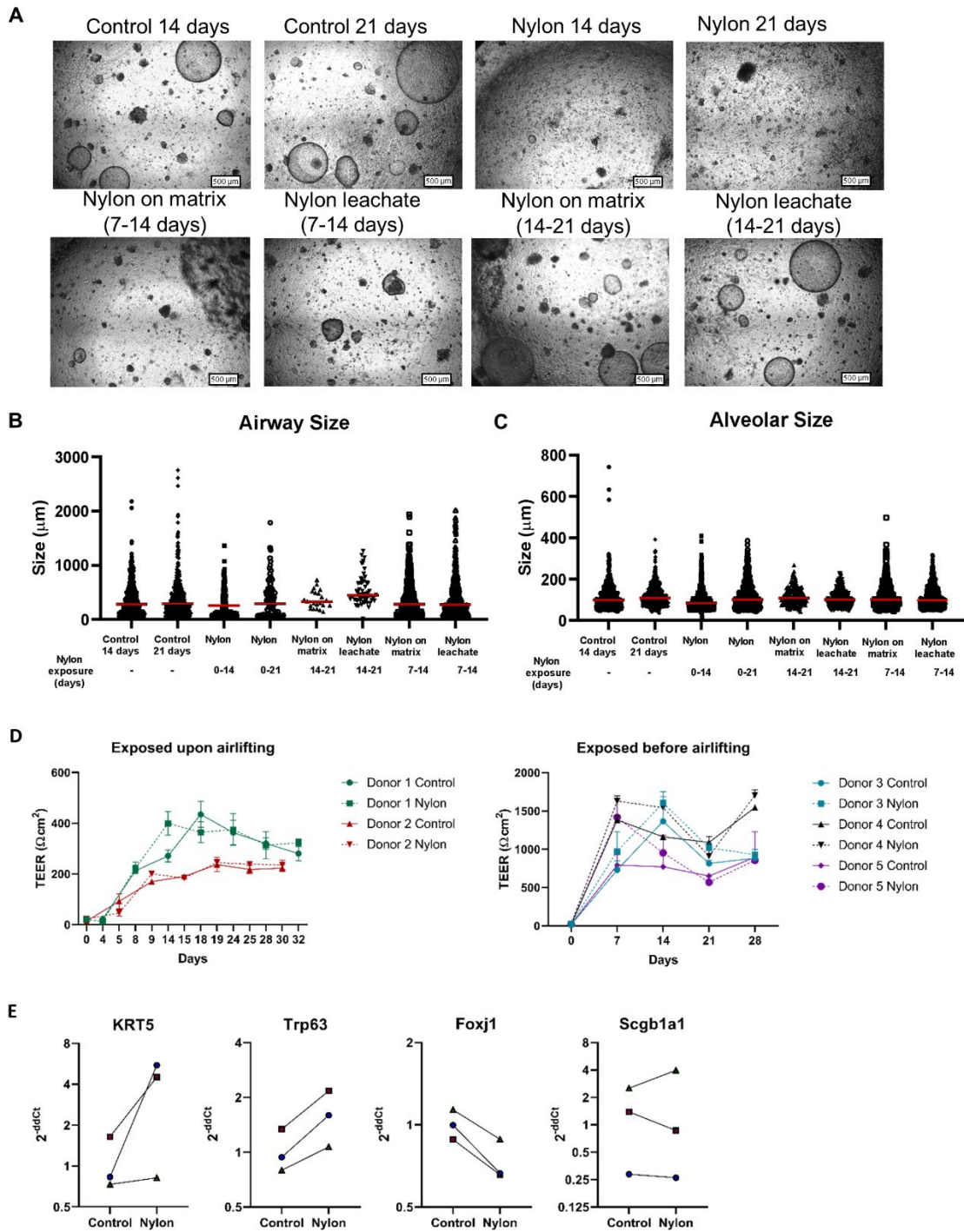


Figure E7. Nylon and its leachate do not affect the size of developing and established lung organoids or the barrier function of air-liquid interface cultures.

(A) Representative light microscopy images of all treatment conditions. (B-C) Quantification of sizes of airway and alveolar organoids following exposure to no or 5000 nylon microfibers or leachate for 7, 14, or 21 days. (n=6). Groups were compared using a Friedman test with Dunn's correction for multiple testing. $P < 0.05$ was considered significant. (D) Effect of 4 weeks basolateral exposure of air-liquid interface cultures to 40-50 $\mu\text{g}/\text{mL}$ 12x31 μm nylon microfibers on their barrier function as measured by the transepithelial electrical resistance (TEER). Cultures were exposed upon or before airlifting. (E) mRNA expression of keratin 5 (KRT5), P63 (Trp63), Foxj1, and Scgb1a1 in air-liquid interface cultures of human primary bronchial epithelial cells (n=3 donors) treated for 4 weeks from the start of culture with 40 $\mu\text{g}/\text{ml}$ 12x31 μm nylon microfibers on the basolateral side.

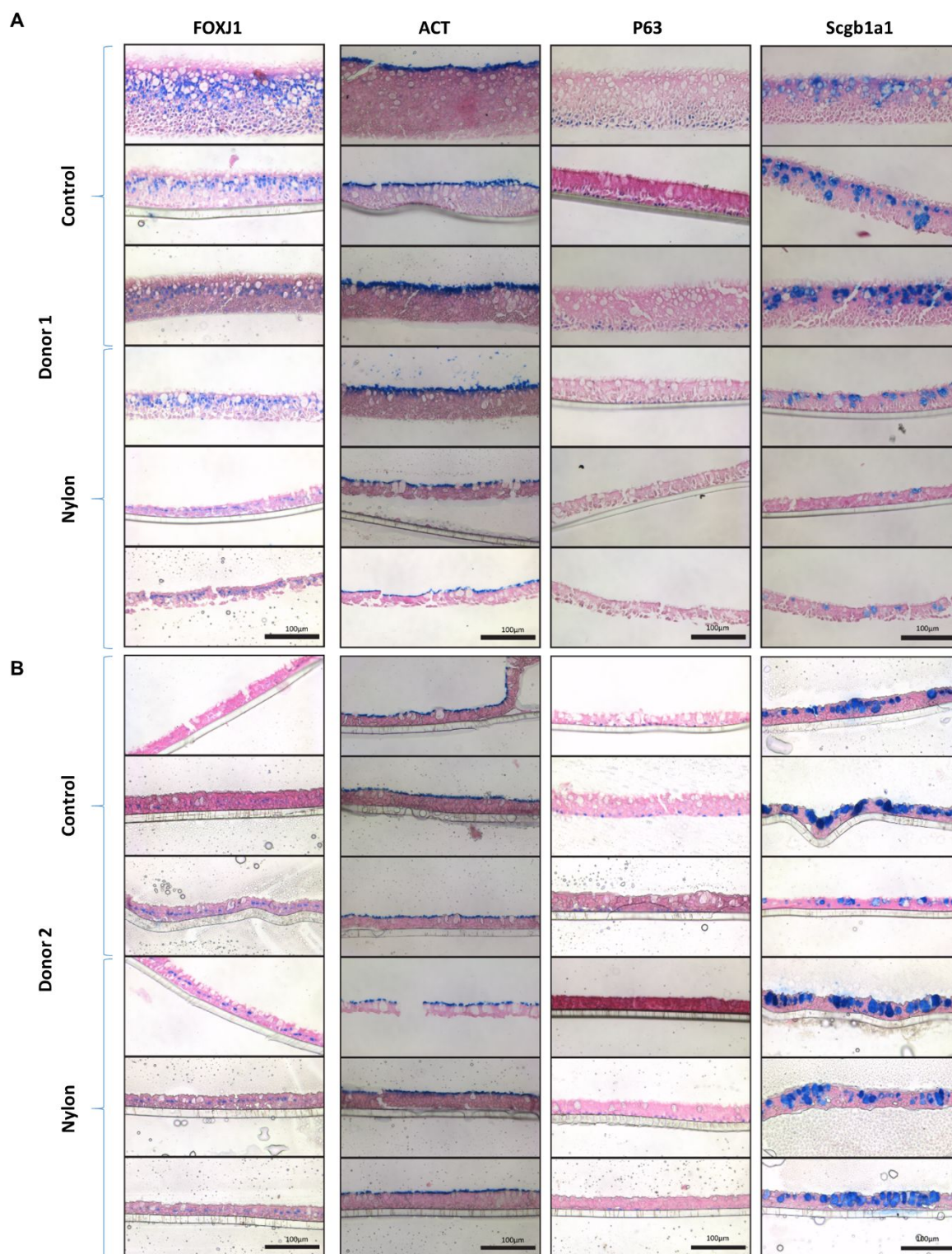


Figure E8. Immunohistochemical stainings for proliferation and differentiation of well-developed (A) and less developed (B) air-liquid interface cultures treated with vehicle or

50 µg/mL 12x31 µm nylon fibers on the basolateral side upon airlifting for 4 weeks. Three technical replicates per donor and condition. Positive staining is blue. FOXJ1 and ACT: ciliated cell markers; P63: basal cell marker; Scgb1a1 = secretoglobin family 1A member: club cell marker.

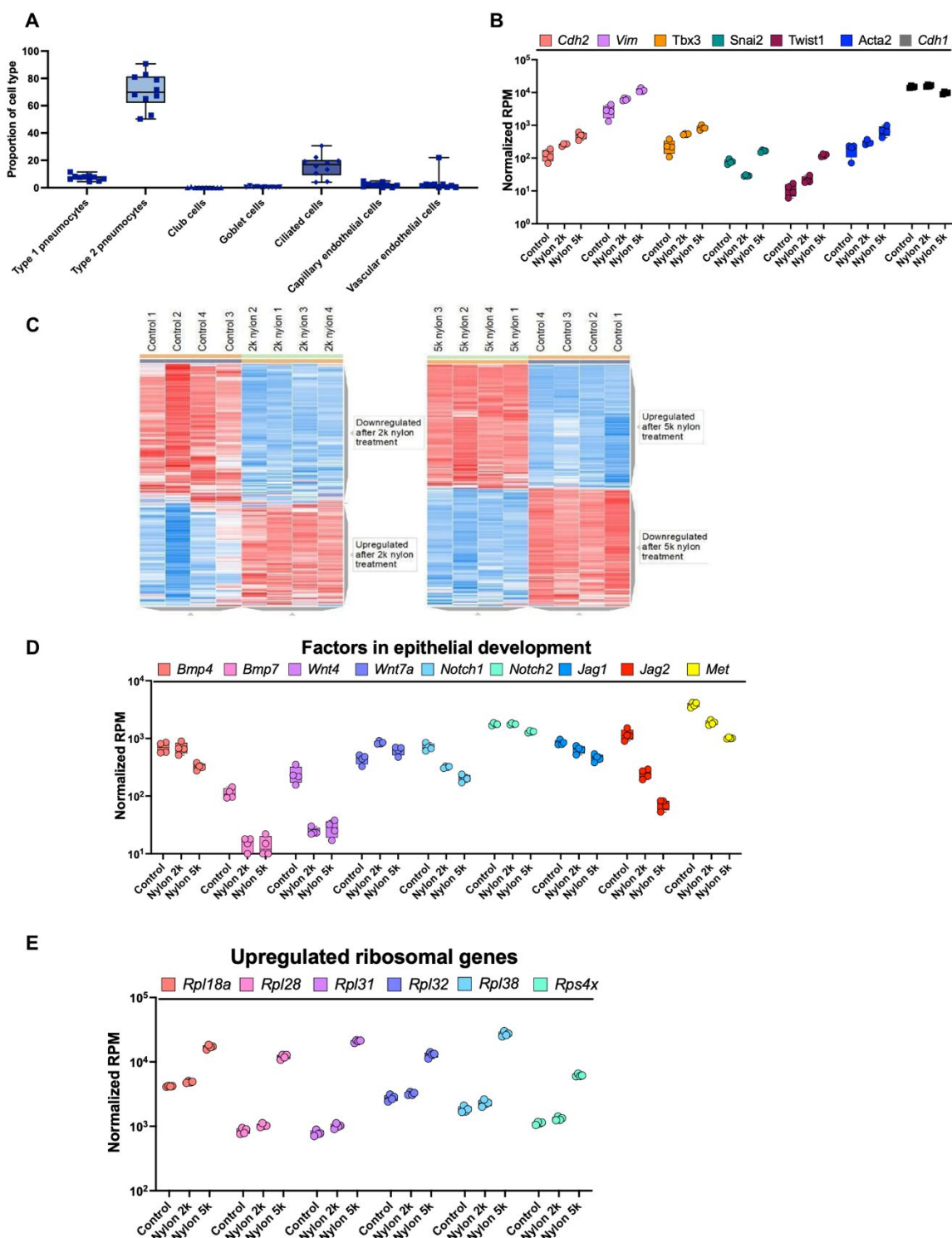


Figure E9. RNAseq analysis of epithelial cells exposed to nylon or not.

(A) Estimated proportions of cell types present in Epcam⁺ cells isolated from murine lung tissue. (B) Expression of EMT markers N-cadherin (Chd2), vimentin (Vim), T-box transcription factor 3 (Tbx3), snail family transcriptional repressor 2 (Snai2), Twist family

BHLH transcription factor 1 (Twist1), alpha smooth muscle actin (Acta2), and of epithelium-specific marker E-cadherin (Chd1) in Epcam⁺ cells isolated from murine lung organoids on day 7 of organoid cultures treated with and without nylon fibers (12x31 μ m). 2k: 2000 nylon fibers per insert; 5k: 5000 nylon fibers per insert. (C) Heatmap of genes differentially expressed by epithelial cells exposed to 2000 nylon fibers (equivalent to 16 μ g/ml nylon) or 5000 nylon fibers (equivalent to 39 μ g/ml nylon) or not. Upregulated genes are marked in red, downregulated genes in blue. Genes were selected with thresholds of fold change >2 and FDR<0.05. (D) Genes encoding factors important for epithelial development. (E) Genes encoding ribosomal family genes.

Table E3: Markers associated with different epithelial populations in lung tissue.

Cell type	Protein name	Gene name
Epithelial cells present in airways		
Basal cells	Transformation-related protein 63	Trp63
	Keratin 5	Krt5
	Integrin alpha-6	Itga6
	Nerve growth factor receptor	Ngfr
Ciliated epithelial cells	Forkhead box J1	Foxj1
	Serine/threonine kinase 11	Stk11
	Acetylated alpha tubulin	Tuba1a
Goblet cells	Mucin 5 subtype B	Muc5b
	Mucin subtype AC	Muc5ac
Club cells	Secretoglobin family 1A member 1	Scgb1a1
	BPI fold containing family A member 1	Bpifa1
Epithelial cells present in alveoli		
Alveolar epithelial cells type I (AECI)	Homeodomain-only protein homeobox	Hopx
	Advanced glycosylation end-product specific receptor	Ager
Alveolar epithelial cells type II (AECII)	Surfactant protein C	Sftpc
	Surfactant protein B	Sftpb

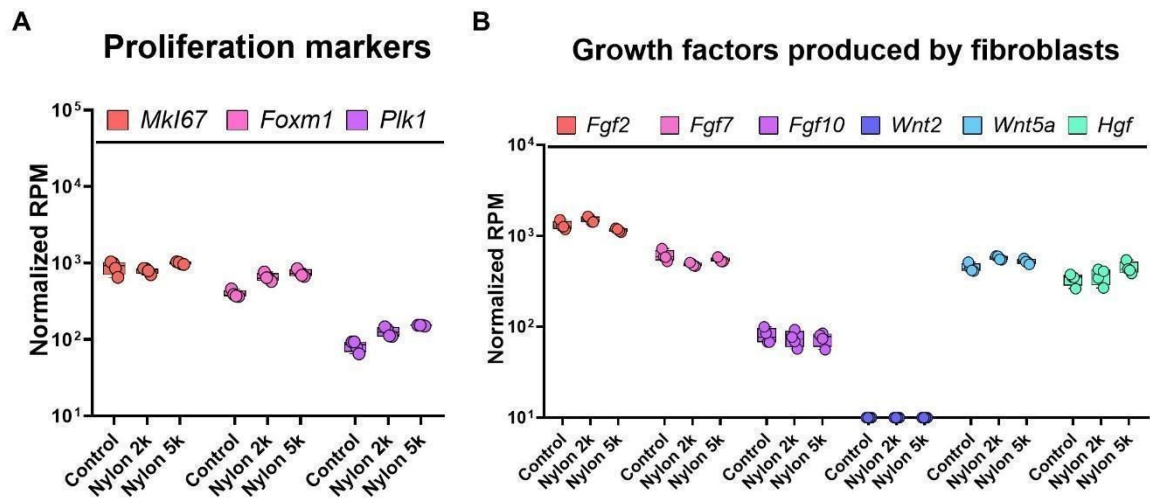


Figure E10. Expression of individual genes in fibroblasts isolated from organoid cultures exposed to nylon microfibers.

(a) Genes associated with proliferation of fibroblasts. (b) Genes encoding factors produced by fibroblasts important for epithelial development (n=4 independent experiments). 2k= 2000 nylon fibers, 5k=5000 nylon fibers.

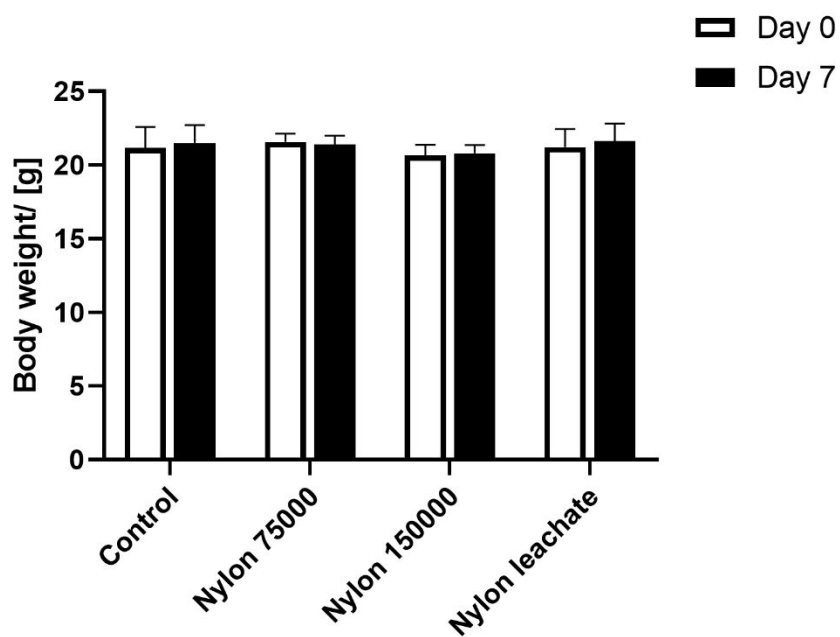


Figure E11. Mouse body weights after exposure to nylon fibers (12x31 μm).

All mice were weighed on day 0 and day 7 (n=8).

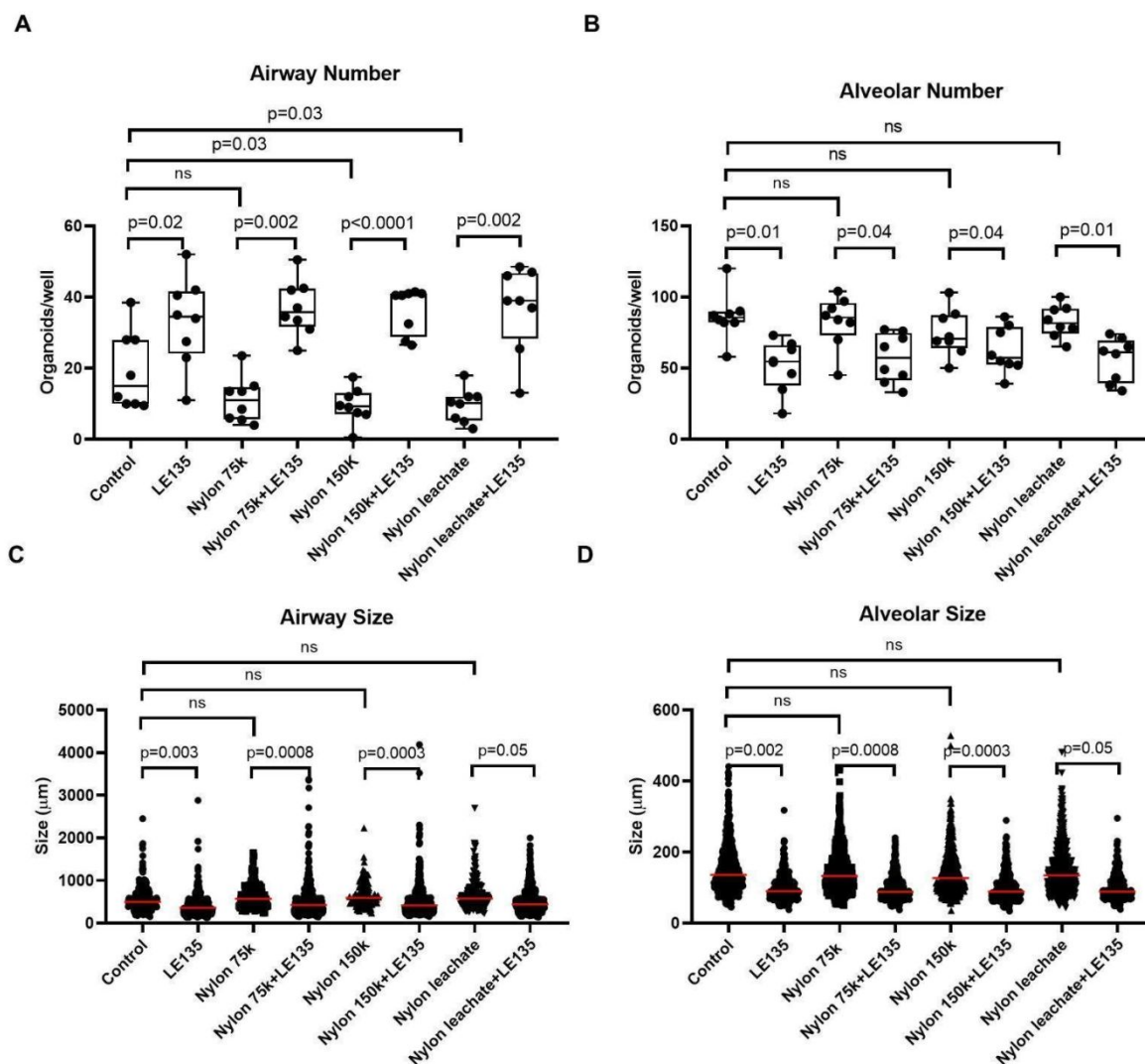


Figure E12. In vivo exposure of mice to nylon fibers results in long-lasting inhibition of airway epithelial differentiation as assessed by organoid formation. Quantification of numbers and sizes airway and alveolar organoids derived from epithelial cells of mice exposed to 75,000 nylon fibers (75k, equivalent to 298 μg nylon) or 150,000 nylon fibers (150k, equivalent to 597 μg nylon) or the equivalent amount of 150k leachate with or without *in vitro* treatment with 5 μM of *Hoxa5* inhibitor LE135 (n=8). The size of nylon fibers is 12x31 μm . (A) Airway numbers. (B) Alveolar numbers. (C) Airway size. (D) Alveolar size. Groups of nylon-treated mice were compared using a one-way ANOVA with a Dunnett's correction for multiple testing. Organoid cultures derived from these mice and treated with LE135 were compared with a paired Student's t test. P<0.05 was considered significant.